HHS Public Access

Author manuscript

Prog Retin Eye Res. Author manuscript; available in PMC 2018 March 01.

Published in final edited form as:

Prog Retin Eye Res. 2017 March ; 57: 108–133. doi:10.1016/j.preteyeres.2016.12.004.

Aqueous outflow - a continuum from trabecular meshwork to episcleral veins

Teresia Carreon[1,2], **Elizabeth van der Merwe**[3], **Ronald L. Fellman**[4], **Murray Johnstone**[5], and **Sanjoy K. Bhattacharya**[1,2,*]

[1]Department of Ophthalmology & Bascom Palmer Eye Institute, University of Miami, Miami, USA

[2]Department of Biochemistry and Molecular Biology, University of Miami, Miami, USA

[3]Department of Human Biology, Faculty of Health Sciences, University of Cape Town, Anzio Road, Observatory, 7925 Cape Town, South Africa

[4]Glaucoma Associates of Texas, Dallas, Texas, USA

[5]Department of Ophthalmology, University of Washington, Seattle, WA

Abstract

In glaucoma, lowered intraocular pressure (IOP) confers neuroprotection. Elevated IOP characterizes glaucoma and arises from impaired aqueous humor (AH) outflow. Increased resistance in the trabecular meshwork (TM), a filter-like structure essential to regulate AH outflow, may result in the impaired outflow. Flow through the 360° circumference of TM structures may be non-uniform, divided into high and low flow regions, termed as segmental. After flowing through the TM, AH enters Schlemm's canal (SC), which expresses both blood and lymphatic markers; AH then passes into collector channel entrances (CCE) along the SC external well. From the CCE, AH enters a deep scleral plexus (DSP) of vessels that typically run parallel to SC. From the DSP, intrascleral collector vessels run radially to the scleral surface to connect with AH containing vessels called aqueous veins to discharge AH to blood-containing episcleral veins. However, the molecular mechanisms that maintain homeostatic properties of endothelial cells along the pathways are not well understood. How these molecular events change during aging and in glaucoma pathology remain unresolved. In this review, we propose mechanistic possibilities to explain the continuum of AH outflow control, which originates at the TM and extends through collector channels to the episcleral veins.

Keywords

Glaucoma; trabecular meshwork; segmental outflow; schlemm's canal; collector channels; deep scleral plexus; distal outflow; mechanosensing; basement membrane; turnover and stability; continuum hypothesis

*Corresponding author: Department of Ophthalmology & Bascom Palmer Eye Institute, 1638 NW 10th Avenue, Room 707A, University of Miami, Miami, USA, 33136, sbhattacharya@med.miami.edu; Telephone: 305-482-4103; Fax: 305-326-6547.

1. Introduction

1.1 Glaucoma and aqueous humor outflow: Overview

Glaucoma is a group of diseases leading to irreversible blindness. The diseases arecharacterized by a pressure sensitive optic neuropathy (Coleman, 1999) with progressive retinal ganglion cell (RGC) death and visual field loss (Coleman, 2003). Worldwide, the resultant silent, painless progressive loss of sight affects over 60.5 million people. This number of people affected continues to increase thereby rendering glaucoma a sight threatening public health problem of broad significance (Quigley and Broman, 2006).

The disease occurs predominantly later in life and typically progresses; however, dysgenesis of the outflow system at times occurs early in life. Manifestations of dysgenesis are present in congenital and juvenile forms of glaucoma but are often not as readily apparent in other glaucoma conditions(Grover et al., 2015). Primary open angle glaucoma (POAG) is the most common form of glaucoma and frequently occurs with elevated intraocular pressure (IOP) (Anderson, 1989; Morrison and Acott, 2003).

Lowering IOP remains a proven intervention, even in normal tension glaucoma (NTG) where IOP remains in the normal range (Anderson, 2003). IOP reduction in NTG generally either delays or halts progression of glaucomatous optic neuropathy (Anderson, 1989). In POAG, inflow rates of aqueous humor (AH) are not increased significantly but outflow facility is decreased (Goel et al., 2010). An aberrantly increased resistance to return of AH to the sytemic circulation likely underlies the IOP elevation.

1.2 Aqueous humor functions

AH is the clear fluid that baths the anterior chamber of the eye. Regulating the balance between aqueous inflow and outflow controls the fluid volume of ocular compartments and maintains IOP. IOP then maintains the shape and related refractive properties of the eye. In addition, AH provides nutrients and removes waste products. AH is actively produced by the ciliary body (CB) epithelium. AH normally exits the anterior chamber (AC) through the filter-like region of the trabecular meshwork (TM) and Schlemm’s canal (SC), finally entering the episcleral veins (EV) (Civan and Macknight, 2004).

Diurnal fluctuations in IOP can occur in normal eyes but are much larger in glaucomatous eyes (Asrani et al., 2000). IOP variations in normal individuals remain within a fairly narrow range and do not result in persistently elevated pressures. Thus, homeostatic mechanisms must exist to regulate IOP in normal individuals. In the pathologic state, these pressure-regulating mechanisms gradually fail. Most likely, molecular changes underlie this functional failure.

1.3 Pathways through the AH outflow system

The pathway for AH to return to the venous system is described as the conventional outflow pathway (Fig. 1A, B). Aqueous passes through the the TM, which is divided into distinct regions: the uveal meshwork, the corneoscleral meshwork, and the juxtacanalicular tissue (JCT). The JCT lies between the last trabecular lamellae and SC inner wall endothelium.

Finally, aqueous encounters the SC inner wall (IW) endothelium. (Fig.1A–D). Aqueous crosses the SC IW endothelium to enter SC either through pores or through transcanalicular conduits arising from SC endothelium. The trabecular meshwork is the proximal portion of the aqueous outflow system. The aqueous flow pathways beyond the TM are collectively termed the distal outflow system. The AH can also exit through other areas described as the uveoscleral pathway, which includes the CB and other structures (Bill, 1989; Bill and Phillips, 1971).

The TM is an essential, and perhaps the most important, tissue mediating IOP regulation. However, the TM does not act in isolation but is a part of a complex organ system dependent on several tissue components working in unison to maintain a homeostatic IOP. Transcanalicular structures traverse SC from SC endothelim and attach to hinged flaps at collector channel entrances (CCE). Signaling pathways that govern both cellular and extracellular behavior determine TM and collector channel mechanical properties. Understanding these cellular signaling pathways is central to delineate normal aqueous outflow regulation and the abnormality in glaucoma.

Identifying flow and tissue motion at the macro level raises questions and provides guidance to explore the detailed geometric relationships and the constituent properties of the outflow tissues. These fundamental questions include details of outflow pathway geometry, cell types, cellular mechanosensory systems, mechanotransduction mechanisms, cytoskeletal responses, signaling pathways, interactions with the extracellular matrix, and elaboration of both the structurally formed and amorphous extracellular matrix. These more fundamental processes will ultimately determine tissue level behavior.

1.4 Article Goals

In this article we first provide a macro view of flow and tissue behavior. This view encompasses the region from initial aqueous entry into the TM to final aqueous discharge into the episceral veins. We consider evidence from both normal and glaucomatous subjects. Our understanding of macro behavior results from visible aqueous humor flow patterns in human subjects. An emphasis is on fluid flow and tissue motion, dynamics that may become abnormal in glaucoma. Second, we will explore studies of tissue pathways as well as cellular and extracellular behavior that determines aqueous flow and tissue motion; we particularly focus on how the tissue pathway and cellular studies can predict and explain pressure-dependent flow and outflow system motion visible at the macro level. We emphasize studies that may provide insight into mechanisms and potential pathways needed for novel therapeutic interventions. Third, we explore how microsurgery may provide insights into AH outflow mechanisms that may aid in improving glaucoma management.

2. Tracking pulsatile aqueous flow from the TM to the episcleral veins

2.1 Pulsatile aqueous outflow patterns

Flow patterns in the aqueous veins (Fig. 2) provide an effective illustration of the aqueous outflow continuum (Asher, 1942; Goldmann, 1946). The tissue continuum from the anterior chamber to the aqueous veins becomes apparent upon recognizing that the TM must transmit

the ocular pulse from the anterior chamber to SC. We propose below an explanatory framework based on observation and experimental data.

Pulstile flow behavior highlights the precise, coordinated responses of tissue pathways that control flow (Ascher, 1961; Johnstone et al., 2011). The original discovery of pulsatile flow reported that flow into the aqueous veins is cyclic and synchronous with the ocular pulse waves that originate in SC (Goldmann, 1946). Recent studies with optical coherence tomography (OCT) document both trabecular and collector channel pulse-dependent motion in vivo (Fig. 3).

The ocular pulse arises through changes in the choroidal vascular volume as the cardiac pulse oscillates between diastole and systole. These choroidal volume changes are characterized as a choroidal piston (Phillips et al., 1992). The ocular pulse can induce pulsatile TM motion outward into the SC causing a decrease in total volume in SC lumen and a transient increase in SC pressure allowing the IOP increase to elicit a pulse wave of AH to leave SC (Fig. 3) (Johnstone et al., 2010; Johnstone et al., 2011).

Including all the tissues in the AH outflow pathways to explain pulsatile flow suggests that flow regulation is not limited to a single location but requires the coordinated behavior of a highly integrated organ system. The entire apparatus is likely regulated at the cellular level to maintain a narrowly defined molecular regime providing tight regulation of IOP homeostasis.

2.2 OCT imaging of TM and CCE wall motion provides pulsatile flow correlates

OCT imaging (Huang et al., 1991) provides a powerful tool to examine both anterior and posterior segment issues in glaucoma (Bussel et al., 2014; Schuman, 2008). Commercial spectral domain (SD-OCT) systems measure structure with a resolution of <10 μm (Fercher et al., 2003). Surprisingly, the Kagemann group demonstrated a decrease in SC area in response to increased IOP using a commercial OCT system in vivo in humans (Kagemann et al., 2010; Kagemann et al., 2012). The OCT imaging of the dynamic outflow system tissue motion had not been feasible previously due to scleral thickness, associated light scattering, and patient motion. These limitations prevented sufficiently rapid image acquisition to detect pulse-induced motion.

To circumvent the limitations of commercial transcleral imaging, an extremely high resolution SD-OCT platform has been developed that images the outflow system with the OCT beam facing the TM surface in ex vivo preparations. TM surface imaging avoids light scattering and vessel shadowing that occurs during scleral surface imaging. The resolution is sufficiently high to permit detailed TM and CCE structures at a resolution similar to scanning electron microscopy (Fig. 4 and 5). As a result, the motion of the aqueous outflow structures and resultant SC and CCE lumen dimension changes have been recently quantified (Xin et al., 2016b).

Cannulating SC and then connecting the cannula to reservoirs at controlled heights provides a hydrostatic pressure head that permits systemically monitoring resultant pressure changes within the canal (Xin et al., 2016b). Dilating SC to study TM motion is the same approach

used during clinical gonioscopy to directly observe blood filling SC. Blood reflux is a surrogate marker for TM motion that results in TM collapse and causes the SC lumen to enlarge. SC pressure reversal in vivo identifies TM motion changes that distinguish normal from glaucoma patients. The high-resolution OCT platform permits real time measurement changes in the lumen dimensions of SC, CCE, and ISCC that occur within milliseconds (Fig. 5).

Dynamic morphologic changes in Fig. 4 & 5 result from a bolus injection of aqueous into SC. A recent study also systematically examined the effect of static reservoir and SC pressures on outflow system morphology. The appearance of the outflow system in Fig. 4 & 5 is similar to that observed with SC pressures in the 30–50 mm range during static pressure measurements (Xin et al., 2016b). Such SC pressures result from normal physiologic activities such as body inversions during yoga and gymnastics (Friberg et al., 1987; Friberg and Weinreb, 1985).

3. Pulsatile aqueous outflow and tissue motion: Implications for IOP regulation

3.1 Pulsatile flow requirement fulfilled by the outflow system

Pulsatile flow requires a chamber, a reservoir, mobile tissue within the reservoir walls, and valve-like inlets and outlets that use cyclic force to generate motion (Johnstone et al., 2011; Levick, 2010; Zamir and Ritman, 2000).

The SC lumen functions as a chamber (Fig. 2, 6, 7). The TM serves as a mobile chamber wall as it distends into SC causing SC lumen dimension changes (Grierson and Lee, 1975a, b; Johnstone and Grant, 1973a; Johnstone and Grant, 1973b). Pulsatile aqueous outflow requires tissue organization at the SC inner wall endothelium to provide one-way flow of AH into SC.

3.2 Valve-like inlets to SC

One-way flow of AH into SC may occur via SC endothelium pores, which have been described (Bill and Svedbergh, 1972; Braakman et al., 2015; Sit et al., 1997). Such pores could provide a one-way inlet into SC. Valve-like structures arising from the SC inner wall endothelium may also act as one-way conduits for flow. These valve-like structures have a lumen, and travel across the SC to attach to the external wall of the canal near the CCE (Bentley et al., 2016; Johnstone, 1974).

We need to further define the organization and and function of these valve-like structures as they relate to overall outflow function. An *in vivo* clinical study demonstrated their attachments to SC endothelium and to SC external wall. The same study demonstrated aqueous discharge from their lumen when they are surgically disrupted.(Johnstone, 2004). Direct *in vivo* observation captured in video recordings demonstrates pulsatile aqueous entry from the AC into their funnel-shaped entrance with the pusle wave passing through a cylindrical portion, finallyentering SC where eddies of blood and aqueous mix.(Johnstone, 2004).

Laboratory experiments performed include light, transmission and scanning electron microscopy to establish the continuity of their wall with SC endothelium and continuity of their lumen with the juxtacanalicular space. The studies also demonstrated the attachments of these valve-like structures to both the TM and SC external wall. In vivo studies in primates demonstrate passage of red blood cells into their lumen from the anterior chamber (Johnstone, 2004) as well as red cell reflux into their lumen from SC. (Johnstone, 1974). Studies have also demonstrated pressure-dependent confirmational changes in their lumen dimensions (Johnstone, 1974). In addition, recent OCT studies demonstrate not only their presence but also their confirmational changes in response to SC pressure changes. These fine tube-like structures were also observed in gross dissections and histologic studies that demonstrate direct connections between the TM and collector channel flaps (Bentley et al., 2016).

3.3 Valve-like outlets from SC

We suggest that physiologic considerations and evidence support the presence of a one-way outlet or checkpoint present at the collector channel entrances at the SC external wall. As the AH from the anterior chamber fills SC, pressure must be lower than that in the anterior chamber to permit AH flow. The reduction in SC pressure that allows entry from the AH into the SC lumen simultaneously requires a one-way mechanism to prevent backflow of the AH into the SC from the episcleral veins. Efforts to characterize the structural features that fulfill the requirements to prevent the backflow of blood into the SC from the collector channels are longstanding (Rohen and Rentsch, 1968).

Recent studies provide further evidence of flap or leaflet-like structures at the CCE (Bentley et al., 2016; Johnstone, 2016) (Fig. 4, 6, 7, 8 & 9) that change shape to prevent backflow into SC (Fig. 4, 5, 8). Studies demonstrated pressure-dependent changes in the CCE shape (Hann et al., 2011; Hann et al., 2014). The CCE shape changes are synchronous with the ocular pulse and can occur in milliseconds (Hariri et al., 2014; Johnstone, 2016).

3.4 Pulsatile flow similarities between lymph and aqueous

The aqueous outflow system has many properties like those seen in the lymphatic system (Park et al., 2014a; Thomson et al., 2014). Tissue turgor is kept within a narrow range by lymphatic homeostatic mechanisms that control the flow of lymph (Levick, 2010). The requirements for pulsatile flow in the AH outflow system are similar to those found in the lymphatic system. Individual segments between valves resemble mini ventricles that act as chambers with an inlet and outlet (Quick et al., 2009; Quick et al., 2007).

Cyclic motion generated by alterations in pulse-induced tissue turgor cause chamber dimensional changes that cause unidirectional fluid flow (Levick, 2010). Evidence indicates that the lymphatics have a dual behavior and can act as either conduits or actively pump against a pressure gradient (Quick et al., 2009). Lymphatic defects can cause ocular hypertension (Thomson et al., 2014). These similarities provide a behavioral link between the aqueous outflow system and lymphatics to return extracellular fluid to the vascular system. Mutations in key proteins, such as LTBP2, present in the TM basement membrane (BM) underlie ocular hypertension and glaucoma (Kuchtey and Kuchtey, 2014).

4. Sites of resistance regulate AH flow

4.1 Proximal and distal resistance

Resistance sites are locations able to act in the regulation of aqueous outflow. Aqueous outflow resistance proximal to the TM is thought to reside primarily in the juxtacanalicular tissue (JCT). The JCT and inner wall endothelium represent key candidates for the TM site of resistance regulation because the spaces in the corneoscleral meshwork may be too large to provide an important site of resistance. Distal resistance requires an additional distinction with regard to its location either distal to the TM or distal to SC.

4.2 Distal resistance: Distal to the TM or SC?

Distal resistance and its relationship to the TM and SC are key considerations to define outflow resistance in glaucoma.. We must determine whether distal resistance means distal to the TM or distal to SC external wall, which represent two distinct mechanisms. The distinction has ramifications for both theoretical constructs for outflow resistance and minimally invasive glaucoma surgical (MIGS) approaches.

If distal indicates distal to the TM inner wall, then TM tissues still may have a central role in resistance, since TM tissues can change their location and configuration. Such resistance changes can occur, since the trabecular tissue distends into SC to occlude SC lumen (Grierson and Lee, 1975b; Johnstone and Grant, 1973a; Johnstone and Grant, 1973b), distends into the collector channels (Lee and Grierson, 1974), compresses SC structures, and reconfigures the CCE at SC external wall through their connections (Johnstone, 2016; Rohen and Rentsch, 1968; Xin et al., 2016a).

If distal refers to only structures that are distal to the SC external wall, then distal resistance alternatives are limited to the CCE and the intrascleral collector channels in the deep scleral plexus (DSP), which course through the sclera to the episcleral veins and the aqueous veins. Identifying the TM, SC, and the distal outflow pathways as possible discrete sites of resistance raises the possiblity that resistance occurs in series. This hypothesis suggests that resistance sites act synergistically with a spectrum of relative inputs that act in concert to synchronously regulate AH outflow and determine IOP (Fig. 2 and 6).

4.3 Experimental perfusion studies identify resistance sites

4.3.1 Chamber deepening during perfusion—Experimental perfusion studies in ex vivo eyes by Ellingsen and Grant lend considerable evidence that resistance is distal to the TM but proximal to SC external wall (Ellingsen and Grant, 1971). In this case, resistance changes result from resistance properties that change SC wall relationships, as assessed through experimental anterior chamber deepening experiments.

Anterior chamber perfusion without iridectomy causes the lens to move backward against the iris. The lens-iris apposition prevents fluid from leaving the anterior chamber, a phenomenon called reverse pupillary block. As a result, the entire lens-iris diaphragm moves backward causing increased tension on the zonules. The zonules, in turn, increase tension on the ciliary body, the scleral spur, and the TM. The entire attachment of the TM to the ciliary

body and scleral spur rotates inward and backward pulling the TM away from SC external wall.

In contrast, perfusion with a needle behind the iris permits fluid to move posteriorly around the lens eliminating reverse pupillary block and no longer results in chamber deepening. When the lens-induced tension on the scleral spur is eliminated, the TM comes into apposition with SC external wall, causing a marked increase in resistance to experimentally induced increases in IOP. This finding is especially striking in glaucoma. When the chamber deepens to hold the TM away from SC external wall, the increased resistance in in response to an experimentally induced change in IOP is completely removed, which strongly implicates SC wall apposition as a cause of resistance in glaucoma (Ellingsen and Grant, 1971).

4.3.2 Experimental removal of the TM or SC external wall followed by perfusion—In the general population, normal IOP is approximately 16 mmHg, and the episcleral venous pressure is 7–8 mmHg. These pressure ranges create a pressure differential across the TM of ~8 mmHg. Early ex vivo microsurgery experiments by Grant maintained an IOP of 25 mmHg, far above the mean IOP under physiologic conditions (Grant, 1958). Subsequent studies by Ellingsen and Grant used perfusion at a range of pressures (Ellingsen and Grant, 1971). Trabeculotomy only eliminated ~14% of resistance when an ex vivo IOP of 5 mmHg (equal to 13 mmHg in vivo) was maintained (Ellingsen and Grant, 1972). Trabeculotomy eliminated 27% of resistance at 10 mmHg (equal to 18 mmHg in vivo) and using higher pressures within the 20–50 mmHg range eliminated 62–82% of resistance.

This work demonstrated that little resistance was eliminated by TM removal at low IOP. These findings were confirmed in a subsequent set of experiments (Rosenquist et al., 1989). In these studies, trabeculotomy reduced resistance by 49% using a similarly low IOP of 7 mmHg and reduced resistance by 75% using a higher 25 mmHg IOP, consistent with a previous report (Ellingsen and Grant, 1971).

In contrast to the pressure increases that occur with increased IOP when the TM moves toward the SC external wall, increasing resistance with increased IOP was completely eliminated even at high pressures when the TM was kept away from SC external wall (Ellingsen and Grant, 1971). Lens depression experiments also demonstrated a highly significant and progressive reduction in resistance as the anterior chamber deepens that in turn causes the TM to move farther away from the SC external wall (Van Buskirk, 1976; Van Buskirk and Grant, 1973).

Systemic perfusions at known pressures followed by fixation using both ex vivo human and in vivo primate eyes demonstrated progressive apposition of the SC walls as IOP increased, typically beginning when IOP rose into the upper teens (Johnstone and Grant, 1973a). Further, TM tissues occlude the SC lumen and the CCE to prevent the AH access to the CCE lumen (Johnstone and Grant, 1973b). Discrete TM regions can also begin to enter the CCE lumen in primate eyes (Grierson and Lee, 1974) with a SC and in bovine eyes with an aqueous plexus (Zhu et al., 2013).

4.4 Evidence indicates distal resistance occurs within the inner third of the sclera

Ex vivo experimental microsurgery studies indicate that the area of the deep scleral plexus in the inner third of the scleral wall of SC (Fig. 2) has the greatest impact on resistance at SC external wall and beyond. A previous study removed two-thirds of the scleral wall of the SC in ex vivo eyes without an appreciable change in resistance. Thus, distal resistance occurs close to the region of the deep scleral plexus (DSP) or collector channels (Grant, 1958).

An excimer laser study also concluded that distal resistance occurs in the region of the deep scleral plexus near SC (Schuman et al., 1999). Most evidence in favor of distal resistance comes from minimally invasive glaucoma surgical procedures (Kaplowitz et al., 2014; Loewen and Schuman, 2013) and the histologic study of glaucoma affected eyes. However, such studies may not provide reliable evidence to provide insight into the physiological mechanisms that control AH outflow (Dvorak-Theobald and Kirk, 1955).

4.5 CCE geometry, mobility and questions of resistance/regulation

The CCE and the ISCC possess a unique geometry. The CCE have hinged flap-like structures at their entrances to permit free movement around their hinged attachment sites (Fig. 2,4,7,8,9), which was first reported by Rohen (Rohen and Rentsch, 1968). The hinged arrangement provides the capability to modulate the AH flow leaving SC (Fig. 2,7,8,9). The ISCC are parallel to, but separated, from SC by long, thin collagenous septa hinged at their junctions with the adjacent CCE (Fig. 2,7,8,9). The hinged arrangement provides a mechanism by which the thin septa can actively move and alter the dimensions of the lumen of the ISCC. Recently, both the CCE and ISCC dynamic dimension changes were demonstrated using OCT (Hariri et al., 2014; Xin et al., 2016a).

The hinged arrangement that creates mobile flaps or leaflets provides a mechanism by which three forces can induce changes in the CCE and ISCC lumen dimensions. The first force occurs through the hinged flap geometry, which provides a means for free movement to permit endothelial cell contractile elements within the walls to actively modulate lumen size (Gonzalez et al., 2013; Gonzalez et al., 2014; Gonzalez et al., 2016; Ko et al., 2016).

The second force arises from the pressure differential between the SC and CCE lumens that can cause changes in lumen size. The differential pressures between the SC and ISCC lumen can also cause septa between the two lumens to move and cause ISCC lumen dimension changes. The structural elements attached between the TM and CCE provide a third force to act at CCE. These attachments create tension on the hinged flaps to alter the lumen size of the CCE and ISCC. Such a tension occurs when the TM moves either radially or circumferentially in relation to SC external wall. Taken together, these forces can act in concert to optimize lumen dimensions.

However, hinged flaps presents a problem when attempting to explain aqueous flow into the CCE from SC. Pressure in the episcleral veins is normally lower than the pressure in the CCE. Mean pressure in the CCE must be lower than the pressure in SC to permit AH flow. Pressure gradients will favor hinged flap movement outward to close the lumen of the CCE and the ISCC as a result of freely moving, hinged leaflets and the mean pressure in these areas.

Rohen recognized the dilemma posed by pressure gradients facing the hinged flaps. His prescient observations first called attention to the presence of hinged flaps, their ability to move, and their attachment to the TM. He proposed that it is necessary to maintain dynamic TM tension, which pulls on the transcleral attachment to permit the CCE flaps to open (Rohen and Rentsch, 1968).

4.6 Collagen-encased ISCC as a resistance site

The external or corneoscleral wall of the SC is composed of interleaving bundles of collagen (Fig. 10 A–D) (Hogan et al., 1971). The CCE and ISCC parallel to SC are encased in this collagenous tissue and have a large lumen relative to their endothelial lining thickness (Fig. 6). The endothelial lining of the ISCC walls attach to the surrounding tissues via integrin attachments. Such considerations make it rather difficult to envision an intrinsic contractile mechanism that could cause a sufficiently large change in the lumen shape to actively modulate AH outflow.

However, the endothelium lining attached to the walls of the SC, the CCE, and the ISCC has perivascular smooth muscle components, which suggest that these regions may possess sufficient contractile components to affect aqueous outflow (Gonzalez et al., 2013; Gonzalez et al., 2014; Gonzalez et al., 2016; Hann et al., 2011; Hann and Fautsch, 2009; Hann et al., 2014; Ko et al., 2016). Such movement is particularly likely given recent evidence that the CCE and ISCC geometry and constituent properties permit free movement in response to pressure changes (de Kater et al., 1992; de Kater et al., 1990; Hariri et al., 2014; Xin et al., 2016a; Xin et al., 2016b).

5. Visible outflow system abnormalities in glaucoma patients

5.1 Pulsatile flow abnormalities

Pulsatile AH outflow requires the coordinated behavior of the outflow system beginning when AH flow enters TM tissues until arriving at the episcleral veins where AH enters the venous circulation (Fig. 2 and 6). A series of pulsatile flow abnormalities are well documented in glaucoma (Ascher, 1949, 1953). As glaucoma pathology advances, pulsatile AH flow diminishes until it is eventually absent (Ascher, 1961; Johnstone et al., 2010).

The AH influx test involves compressing the episcleral veins distal to the aqueous vein complex. This compression causes an increase in the pulsatile flow proximal to the point of compression (Ascher, 1944). Small tributary episcleral veins join larger aqueous vein pathways before reaching their episcleral venous destination to discharge AH into the venous system. The tributary episcleral veins typically are in an oscillatory pressure equilibrium with the aqueous veins (Ascher, 1942; Johnstone et al., 2011). Oscillatory blood enters from the tributary episcleral veins into the aqueous vein during the diastolic phase when aqueous vein pressure is low.

Blood entry stops when the aqueous vein pressure becomes higher than the pressure in the tributary vein during the systolic phase. When the AH flow is regionally blocked downstream in the lower pressure episcleral veins aqueous discharge into the vein is prevented. Increasingly vigorous pulsatile AH flow waves develop and spread into the more

proximal tributary episcleral veins. These tributary episcleral veins containing tributary blood normally maintain the same mean pressure as the aqueous veins, because they are in an oscillatory equilibrium. The entrance of aqueous into these tributary vessels suggests that outflow system structures are able to increase pulsatile pressure gradients in response to a regional increase in episcleral venous pressure. Furthermore, AH flow into the tributary episcleral veins can only occur if a mechanism at the level of the SC increases the pulse wave pressure in SC to then cause increased AH flow into the upstream blood-containing episcleral tributaries.

However, compression of downstream episcleral veins does not result in more vigorous pulsatile flow in glaucoma patients. Blood instead refluxes from the surrounding blood containing episcleral tributaries and fills them to the level of the aqueous vein scleral emissaries where they arise from the sclera. The mechanisms that normally permit increased pulsatile flow when EVP pressure increases do not function in the glaucomatous outflow system (Ascher, 1961).

The compensation maximum test involves increasing IOP by applying a measured pressure on the eye surface with an ophthalmodynamometer. Pulsatile flow increases markedly in normal subjects, while the same pressure causes pulsatile flow to decrease or stop altogether in glaucomatous eyes. The pressure necessary to stop pulsatile flow correlates with glaucoma severity (Kleinert, 1951; Stambaugh et al., 1954).

5.2 TM motion abnormalities in glaucoma

5.2.1 Histology studies following in vivo fixation with IOP<EVP—Blood reflux into SC is used as a surrogate for TM motion. The SC lumen is more than a potential space when IOP is within the normal range. Reversal of the pressure gradients between the anterior chamber and SC causes the TM to move away from SC external wall to enlarge the SC lumen as shown in vivo fixation in the living eyes of primates (Grierson and Lee, 1975b; Johnstone and Grant, 1973a). The studies also demonstrate that blood enters the canal from the episcleral veins (Johnstone, 1974, 2004), as blood enters the canal with pressure gradient reversals as small as 4 mm Hg (Johnstone et al., 1980).

5.2.2 Gonioscopy studies when EVP is greater than IOP in vivo in normal humans—Gonioscopy is a technique that permits direct observation of the TM in human subjects. The transparency of the TM permits easy observation of blood entry into SC. Studies in living primate eyes followed by histology demonstrate that the TM actively moves when it fills with blood (Grierson and Lee, 1975a, b; Johnstone and Grant, 1973b) (Fig. 5). These *in vivo* observations demonstrate that blood reflux and TM motion are consistant with the direct motion observed in human subjects.

Several techniques have been used in studies exploring SC blood reflux in humans. Pressure reversal in human subjects causes blood to reflux into SC in vivo by raising episcleral venous pressure through jugular compression or with a goniolens to compress the episcleral veins (Schirmer, 1971; Smith, 1956; Suson and Schultz, 1969). Body inversion also causes an episcleral venous pressure increase with concomitant SC pressure reversal (Weinreb et al., 1984) and blood reflux (Friberg et al., 1987; Friberg and Weinreb, 1985). An alternate

method to achieve SC blood reflux is external globe compression (Ascher, 1961) or aqueous withdrawal (Kronfeld et al., 1942) to a level where IOP is below EVP.

5.2.3 TM movement when EVP is greater than IOP in normal and glaucoma subjects—In normal subjects, the pressure gradient reversal causes SC filling to begin in 5–10 seconds and to finish in 15–30 seconds. A similar rapid elimination of SC blood restores normal pressure gradients (Schirmer, 1971). Initially, SC fills rapidly and completely (Schirmer, 1969, 1971). As glaucoma progresses, progression of manifestations of TM motion failure can occur.

In ocular hypertension, rapid SC filling slows, although the canal eventually fills with minimal impairment to the outflow facility (Schirmer, 1969, 1971; Suson and Schultz, 1969). As glaucoma progresses with deteriorating outflow facility, filling defects appear, and the SC no longer fills completely with blood (Kronfeld, 1949; Suson and Schultz, 1969). In more advanced glaucoma, SC blood reflux fails to occur, even when aggressive measures are implemented to reverse pressure gradients (Kronfeld, 1944, 1949; Suson and Schultz, 1969).

6. ECM of the TM determines TM motion and stiffness

6.1 ECM composition, turnover and alterations in glaucoma

The extracellular matrix (ECM) composition differs widely and is divided into 1) highly organized structures such as the TM lamellae, 2) basement membrane (BM) that forms a continuous layer beneath cell membranes that underlie the trabecular lamellae endothelim and 3) amorphous ECM located in structures such as the juxtacanalicular space. Numerous structural proteins and proteases mediate ECM turnover and stabilization. Molecular and protein changes that occur in the ECM at the transcriptional and translational levels cause fluctuations in pressure and resistance (Keller et al., 2009a; Keller et al., 2009b; Keller et al., 2008).

Alterations in various ECM proteins including proteoglycans, collagens, and actins can occur. The functions of these proteins determine the changes that will occur in the ECM after alteration. For example, collagens and actins establish the protein polymeric framework of the ECM. Glaucoma induces alterations in gene expression of ECM proteins, such as cochlin, matrix gla protein, type V collagen, MMP-1, and MMP-10 (Vranka et al., 2015b).

One of the most extensively studied ECM protein groups is matrix metalloproteinases (MMPs), which are proteinases responsible for ECM degradation. The MMPs are produced as zymogens or inactive forms, and are converted later into the active form of the enzymes. The Mammalian Degradome Database (Perez-Silva et al., 2016) identified 23 related MMPs in humans, and reports document the presence of several MMPs in the TM.

These proteases participate in the maintenance of outflow facility. The protease ability to cause ECM turnover or structural protein degradation determines the specific roles. Higher MMP levels increase outflow, while MMP inhibition decreases outflow (Bradley et al., 2001; Keller et al., 2009a). A thorough investigation of MMP and total proteases function is still lacking in both the TM region and the entire outflow system.

6.2 Insights and gaps in knowledge related to ECM regulation mechanisms

6.2.1 Proteases—Although the Mammalian Degradome Database has provided useful information, examinations into the proteases specific to TM tissue are limited and warrants further study. While extra-long lived proteins (ELLP) have been investigated to some extent using pulse labeling and mass spectrometry (Savas et al., 2012; Toyama et al., 2013), a thorough investigation into short lived proteins is still lacking. We must determine the functional relevance of multiple enzymes and evaluate their effects on the AH outflow system using targeted genetic manipulations.

Mechanical stretching can increase MMPs, such as MMP14 and MMP2, but decrease MMP inhibitors, such as tissue inhibitor of metalloproteinase 2 (TIMP2) (Bradley et al., 2001; Keller et al., 2009a). Overall, MMPs are ECM components that likely contribute to the maintenance of outflow homeostasis. Further investigation in this area, particularly high throughput stable isotope based degradation and stability analyses, promise to reveal new insights to expand our understanding.

6.2.2 Glycoproteins and Proteoglycans—Glycoproteins and proteoglycans are the predominant proteins present in both the ECM and BM. The heavily glycosylated proteoglycans can play several roles including fluid channeling, so these proteoglycans can modulate flow pattern regulation. The sugar or glycosaminoglycan (GAG) side chains were intially thought to modify outflow resistance. A major proteoglycan in the TM ECM is secreted protein acidic and rich in cysteine (SPARC).

In particular, SPARC is the most highly expressed gene product in the TM (Haddadin et al., 2009; Swaminathan et al., 2013). In SPARC KO mice, a substantial decrease (up to 20%) in the mean IOP accompanies this AH outflow increase. The outflow increase occurs uniformly 360° degrees around the TM circumference (Haddadin et al., 2009; Swaminathan et al., 2013). Targeted disruption of the TSP1 and TSP2 genes yielded similar results in mice (Swaminathan et al., 2014).

Targeted disruption of other matricellular proteins, such as SPARC (Haddadin et al., 2009; Swaminathan et al., 2013; Swaminathan et al., 2014) and Thrombospondin-1 and 2, produce a more uniform flow of AH (Haddadin et al., 2009; Haddadin et al., 2012). Plaques, microfibrillar materials, and matricellular proteins observed in glaucomatous TM likely alter the uniformity of AH flow.

Cochlin is an extracellular matrix protein with mechanosensing capabilities that has been recently identified in the TM. Cochlin deposits are present in the outflow system of glaucoma patients at locations where aqueous outflow resistance occurs (Bhattacharya et al., 2005b; Vranka et al., 2015a).

Another large proteoglycan, versican consisting of various GAG side chains is unevenly distributed in the TM region. Versican distribution inversely correlates with AH outflow rates (Keller et al., 2009a; Keller et al., 2008; Vranka et al., 2015b). Hyaluronan, another proteoglycan, can also influence outflow resistance (Keller et al., 2009a; Keller et al., 2012). Simultaneous hypo- and hyper-glycosylation occurs in the glaucomatous TM compared to

controls (Sienkiewicz et al., 2014). However, a comprehensive analysis of proteoglycan levels and their glycosylation states in the TM has not been done.

6.3 The juxtacanalicular space, ECM and glaucoma

The juxtacanalicular space can accumulate significant quantities of ECM material. Microfibrillar materials (Rohen et al., 1993; Rohen et al., 1985), deposition of specific extracellular matrix (ECM) proteins (Bhattacharya et al., 2005b; Vranka et al., 2015a; Vranka et al., 2015b), and proteinaceous mucopolysaccharide deposits are found in the TM of glaucoma eyes (Freddo, 1993; Tektas and Lutjen-Drecoll, 2009). In addition, the TM and SC can contain sheath derived plaque material and microfibrillar deposits (Lutjen-Drecoll, 1972, 1973, 1999, 2000; Lutjen-Drecoll and Barany, 1974; Lutjen-Drecoll et al., 1972; Lutjen-Drecoll and Eichhorn, 1988; Lutjen-Drecoll et al., 1981; Lutjen-Drecoll et al., 1986; Rohen et al., 1993; Rohen et al., 1985). Slight quantitative differences in this ECM material were found when comparing untreated or medicated glaucomatous subjects (Lutjen-Drecoll et al., 1986; Rohen et al., 1993; Tektas and Lutjen-Drecoll, 2009), yet the overall ECM material is significantly different between normal control and glaucomatous eyes (Rohen et al., 1993; Tektas and Lutjen-Drecoll, 2009).

6.4 Implications of ECM abnormalities that alter tissue stiffness in glaucoma

Biomaterial properties, such as stiffness as reflected by the elastic modulus, is significantly increased in the glaucomatous TM (Last et al., 2011). Elevated levels of proteoglycans or changes in their glycosylation status can alter stiffness. Whether the low flow regions also have higher level of proteoglycans and/or different sugar side chains are questions for future investigation.

The specific ECM composition of high and low flow areas remains unresolved. Such investigations are necessary to determine the relationship between flow rates and TM stiffness since low flow regions have increased TM stiffness compared to high flow regions (Ethier, 2016). Investigations of stiffness between normal and glaucomatous TM (Morgan et al., 2015; Russell and Johnson, 2012; Vranka et al., 2015a) combined with the stiffness of the high and low flow regions will give new insight into AH resistance in the TM; in particular, identifying the spatiotemporal molecular changes associated with the increased resistance of the TM tissues (Morgan et al., 2015). Current developments in high throughput approaches (Savas et al., 2012; Toyama et al., 2013) will be likely to provide important, fundamental insights.

6.5 ECM interactions in pathways across SC endothelium: funneling and pores

Some studies suggest that the JCT and SC regions provide the major sources of resistance to AH outflow that cause IOP elevations in glaucoma. One hypothesis is that cells present in the TM and SC inner walls may produce a convergence known as “funneling” of the AH through the JCT to promote the exit of AH through pores present along the SC inner wall endothelium (Johnson et al., 1992; Stamer and Acott, 2012). The funneling itself may generate resistance that contributes to the overall segmental nature of AH flow (Johnson et al., 1992; Stamer and Acott, 2012). Pore characteristics, such as pore density and pore

formation, may impact overall resistance. Glaucomatous eyes may have a lower pore density and impaired pore formation (Braakman et al., 2015; Stamer and Acott, 2012).

6.6 Segmental flow through the TM

Many factors contribute to segmental outflow that modulate IOP homeostasis (Chang et al., 2014; Goel et al., 2010; Stamer and Acott, 2012). Some of these factors are affected by the pathological changes in the low flow regions of glaucomatous eyes described in the literature. Outflow resistance resulting from ECM changes, matrix metalloproteinases, cytoskeletal changes, and BM alterations are all potential factors that contribute to segmental outflow.

In addition to segmental flow, high and low flow regions have been identified in the trabecular meshwork. Non-uniform aqueous flow around a 360° circumference of the the TM suggests that high and low flow regions may change in a time dependent fashion (Stamer and Acott, 2012). Although the actual reorganization of these regions has not been described, evidence suggests that high and low flow regions contribute to the segmental flow through the TM. Persistant changes in these regions could contribute to glaucoma pathology (Buller and Johnson, 1994; Stamer and Acott, 2012).

7. Mechanosensory structural components of the AH outflow system

Here, we review the various components of the anterior chamber that underlie its structural composition and mechanosensing properties. We also discuss aqueous outflow properties in cardiovascular and lymphatic systems for comparison.

7.1 Basement membrane importance in the aqueous outflow system

The BM forms a continuous layer overlying cell membranes in any given region and is often characterized as a thin yet dense structure. The BM is composed of various protein fibers and GAGs that function cooperatively to separate the epithelium from the adjacent tissue. Although termed a “membrane”, the BM is not a true membrane, as it lacks a lipid bilayer, a defining feature of membranes. The BM term was coined in 1938 following electron microscopic observations (Kalluri, 2003). Despite the misnomer, the term remains in common use. A BM lines the trabecular lamellae. A thin, discontinuous BM also lines the endothelial lining the trabecular wall of the SC. A more robust BM lines the external wall of SC and the collector channels.

7.2 Basement membrane dynamics and angiogensis

Maintanance of the vasculature is a dynamic process that requires growth, degradation, or pruning. The initial step for vascular growth is overcoming the physical barrier imposed by the BM (Warren and Iruela-Arispe, 2014). Vascular BM components initiate and terminate angiogenesis. During the initial step in angiogenesis, the BM must change into a ‘soft gel’ composition to form functional capillaries for neo-vessels to develop (Clark and Clark, 1938). This composition is the provisional BM and differs from the assembled or homeostatic stationary BM.

Endothelial cells dislodged from existing blood vessels migrate and become surrounded by ‘provisional matrix’, which provides proliferative cues. Further in the process, subsequent changes in the BM structure create an ‘assembled matrix’ to provide growth-arresting cues (Form et al., 1986; Madri, 1997). Secreted proteases control BM degradation for multiple purposes: the liberation of cells (usually endothelial cells in the vessels) from their cell-surface anchors (integrins), the release of growth factors (VEGF, bFGF, PDGF, etc.), and the detachment of pericytes (Folkman and D’Amore, 1996). This degradation exposes cryptic protein domains with pro or anti-angiogenic functions (Prockop and Kivirikko, 1995; Xu et al., 2001). The BM within different organs can vary in composition, expressing major protein components such as Collagen IV, SPARC, Nidogen, and Perlecan in different quantities (Bhattacharya and Carreon, 2015; Candiello et al., 2010).

7.3 Basement membrane changes in glaucoma

BM ultrastructure looks identical under the electron microscope, which complicates identifying visual distinctions in the actual composition of the BM at any given time. So, the BM within two regions of the same organ may not be identical but differences may not be idenified even with repeated examinations (Halfter et al., 2015; Uechi et al., 2014). Aging also greatly affects the BM composition, as it undergoes significant alterations to increase thickness (Fig. 11 A–D) and alter composition (Candiello et al., 2010). BM studies of primary open angle glaucoma (POAG) and control eyes used an equal distribution of genders among age group 55–59 (Fig. 11E). These studies revealed significant BM thickening in glaucomatous eyes beyond that caused by ageing alone (Fig. 11F), which further corroborates the dynamic composition of the BM.

However, previously studies found no differences between the BMs from POAG and normal eyes (Hann et al., 2001). These studies examined only POAG samples and could not demonstrate differences observed in other forms of glaucoma. Other reports found the presence of type IV collagen in the TM and SC (Kizhatil et al., 2014; Picciani et al., 2007a; Picciani et al., 2007b). Prior ultrastructure studies demonstrated the accumulation of BM-like material staining for type IV collagen in steroid-induced glaucoma. These specific studies found fine fibrillary material in the subendothelial region of the TM deposited just underneath the SC inner wall endothelium (Tektas and Lutjen-Drecoll, 2009).

In contrast, this fibrillary material adheres to the sheath of elastic fibers in the SC region in POAG eyes. The differences in accumulation and adherence patterns demonstrates that differences in BM alterations occur in different types of glaucoma (Tektas and Lutjen-Drecoll, 2009). Further investigation into glucocorticoid treatment with dexamethasone demonstrated a more continuous BM below the inner wall of the SC in both human and mouse eyes following treatment (Overby et al., 2014). These findings indicate altered BM processing in glaucoma compared to controls (Rohen et al., 1993; Rohen et al., 1985; Tektas and Lutjen-Drecoll, 2009).

7.4 Basement membrane composition and mechanosensing

A number of BM proteins are also found in the BM of the tectorial membrane and in ruffle membranes involved in mechanosensing, which suggests they could also reside in the BM of

the TM. We identified α-tectorin and its interactors (Gasdermin, Wolframin) (Goel et al., 2012) and Cathepsin F (CTSF) in the BM of the TM. CTSF was detected in the retinal BM (Candiello et al., 2010). A number of these proteins also express syn with the extracellular matrix protein cochlin, and in silico analyses suggest their possible interaction with cochlin (Fig. 12).

Identifying these BM proteins raises the question of whether fine mechanosensing regulation can modulate BM matrix stability and turnover. Indeed, a study identified significant differences in type IV collagen patterns (Picciani et al., 2007b). However, the the inability to explain the distinct differences in staining patterns from using different collagen antibodies (Fig. 10 A–C), resulted in elimination of the immunostaining from the published report (Picciani et al., 2007b).

Polyclonal type IV collagen antibody using western blotting clearly showed more degraded protein in the normal TM compared to that in POAG (Fig. 10D). The linear mode in matrix assisted laser disruption ionization-time of flight (MALDI-TOF) analyses of isolated BM material from the TM showed more intact Wolframin in the BM from POAG than in controls (Fig. 10E), consistent with the previous analyses of these proteins in the TM (Goel et al., 2011) (Fig. 10F). These findings are consistent with reduced BM protein degradation or more intact BM proteins in the glaucomatous TM.

Type IV collagen synthesis and folding also depends on the hydroxylation of prolines and lysines by prolyl hydroxylases, lysyl hydroxylases (Prockop and Kivirikko, 1995), and lysyl oxidase-like protein-2 (LOXL2) that contributes to the regulation of neovascularization (Bignon et al., 2011). After vessel formation, anti-angiogenic peptides are released, to stimulate arrest and stabilization of the formed vessel.

LOXL1 and LOXL2 are implicated in glaucoma and may underlie the different surgical outcomes in glaucoma (Park et al., 2014b; Thorleifsson et al., 2007; Van Bergen et al., 2013). Type IV BM is referred to as assembled BM (Kalluri, 2003). In the vasculature, the podosomes often control degradation of the extracellular matrix and promote invasive cell migration (Warren and Iruela-Arispe, 2014). Reduced podosomes have been observed in TM cells with low outflow (Keller et al., 2009b) and in glaucomatous nee mice (Mao et al., 2011). These findings implicate reduced degradation in the glaucoma process.

7.5 Down-regulation of basement membrane degradation in glaucoma

A number of BM proteins have been identified using stable isotope labeling, imaging, and mass spectrometry in different organs, including the tectorial membrane of the inner ear (Lechene et al., 2006; Zhang et al., 2012). Some BM components are poorly captured by conventional protein extraction methods, as some mutations in low abundance BM proteins, such as LTBP2, arise during ocular hypertension (Kuchtey and Kuchtey, 2014).

Several labs have now developed methods to capture low abundance BM proteins (Patel et al., 2008; Uechi et al., 2014). To confirm newly identified proteins as BM proteins, the following methodology is recommended: search in Uniprot (www.uniprot.org), Matrix database (http://matrixdb.ibcp.fr/), and in silico analyses to determine matrisome protein

domains in the identified proteins (http://matrisomeproject.mit.edu/). If the protein is captured in the BM and is also found in these databases, it most likely occurs in the BM of interest. The last database is based on in silico analyses of domains found in BM proteins and can strongly implicate the protein as a BM component.

Mechanosensors transduce biomechanical forces, such as shear stress and mechanical stretching. These transducers act as regulators of vascular homeostasis in tissues experiencing fluid flow (Deng et al., 2014). New vessel formation from the pre-existing vasculature is a feature of development and is more tightly regulated in adulthood. The distinctions between developmental and adult vascular sprouting remain undetermined. In tissues experiencing fluid flow, biomechanical forces regulate vascularization. Neovascularization in adults may occur by non-angiogenic expansion of preexisting vessels. This process is most affected by biomechanical forces including shear stress (Kilarski et al., 2009), but other biomechanical forces can also affect new vessel formation.

7.6 Mechanosensing in aqueous outflow and vascular pathways

Mechanotransduction of shear stress and mechanical stretching represent well-studied mechanisms to maintain homeostatic setpoints in the cardiovascular and lymphatic systems. The IOP in normal eyes undergoes large diurnal fluctuations. Since the TM is a region that provides resistance, the TM must sense shear stress and mechanical stretching associated with flow, as well as the variations in flow. Although the volume of AH flow is much less compared to other circulatory system fluids, the TM seems capable of responding to AH flow changes.

As investigations of the outflow system continue, similarities between the aqueous outflow system and other circulatory systems becomes increasingly apparent. Segmental cochlin deposits in parallel with segmental outflow resistance occur in human POAG samples (Bhattacharya et al., 2005c; Goel et al., 2012) and in the DBA/2J mouse model of glaucoma (Bhattacharya et al., 2005a). Although, the DBA/2J mouse model is typically used as a model for optic nerve damage in primary open angle and pigmentary glacuoma, approximately 5.3 percent of these mice have little to no pigment dispersion and have an open angle with elevated IOP. These mice are used as “pure ocular hypertensive” models for about 20 days between 8–9 months of gestation (Wang et al., 2015).

7.6.1 Cochlin multimerization induced by mechanotransduction—Cochlin deposits are also associated with deposits of mucopolysaccharides distributed in a segmental pattern in pathologic TM tissues (Bhattacharya et al., 2005c). Cochlin undergoes multimerization following shear stress or mechanical stretching (Fig. 13A) and under high divalent ion concentrations (Bhattacharya et al., 2005b; Goel et al., 2012). These two conditions in combination create an environment that favors cochlin multimerization.

Cochlin is a secreted protein that contains a signal peptide (SP), two von Willebrand factor A-like domains (vWFA1 & vWFA2) (Bhattacharya, 2006), and two sites that undergo glycosylation (Fig. 13B; indicated by G) (Robertson et al., 2003). The von Willebrand factor (vWF, in particular von Willebrand factor A (vWFA)) in vascular tissues acts as a

mechanosensor that responds to shear stress through proportional multimerization to induce distinct interactions with different protein interactors (Stockschlaeder et al., 2014).

7.6.2 vWFA multimerization determines mechanosensory responses— Extensive multimerization occurs in the glycoprotein vWFA under various conditions, including high shear stress (Fig. 13C). The vWF plays an essential role to maintain normal hemostasis. Hydrodynamic shear performs a regulatory role in vWF self-association and multimer formation (Schneider et al., 2007; Shankaran et al., 2003; Shankaran and Neelamegham, 2004; Siedlecki et al., 1996) promoting a range of complex biological responses, including shear-induced platelet activation (Moake et al., 1986; Savage et al., 2002). The degree of multimerization determines binding to different proteins to elicit different mechanosensory responses.

The human vWF gene codes a large precursor polypeptide consisting of a 22 amino-acid signal peptide (SP), a 741 amino acid propeptide, and a mature subunit of 2050 amino acids that serves as a basic monomer. The vWF contains up to 22 carbohydrate side chains. It is processed into a mature 220 kDa monomeric unit after biosynthesis. vWF then undergoes posttranslational modifications for example, glycosylation, dimerization, and multimerization (Fig. 13D).

The vWF multimers exist in low, intermediate, high (HMWM), and ultra large molecular weight (MW) sizes (Fig. 13C). The ultra large MW (ULMW) vWF is >10,000 kDa and usually exists in the Weibel-Palade bodies in endothelial cells or in α-granules of megakaryocytes (Sporn et al., 1987). The functional roles of different vWF multimers vary based on protein-protein interaction. ULMW multimers do not have physiologic activity.

HMW multimers are most effective in platelet activation and hemostasis under high shear stress (Fig. 13C). The HMWM have the highest binding capacity for collagen and the platelet receptors glycoprotein (GP) Ib, IIb, and IIIb. This property promotes platelet adhesion and aggregation after vessel damage and under conditions of high fluid shear stress (Moake et al., 1986; Savage et al., 1996; Schneider et al., 2007; Sporn et al., 1987).

Normal hemostasis depends on the regulation of VWF multimer size by ADAMTS13. ADAMTS13 cleaves the endothelial cell-bound ULMW vWF multiple times into shorter multimers under conditions of high fluid shear stress (Shim et al., 2008) to produce factor FVIII, platelets, GPIbα, and TSP-1 (Skipwith et al., 2010). The A2 domain in vWF contains the cleavage site (Fig. 13D), which is exposed under normal shear conditions as a result of the three-dimensional changes in the vWF structure (Siedlecki et al., 1996).

Excessive proteolysis of vWF severely compromises hemostasis with low circulating vWF HMWM. Yet, lack of ADAMTS13 causes an abnormal accumulation of ULMW leading to spontaneous platelet aggregation and thrombotic thrombocytopenic purpura. A concomitant loss of vWF functions, such as binding with collagen, ristocetin, and factor FVIII (VWF:CB, VWF:RCo, and VWF:FVIII), may correlate with a progressive decrease in vWF multimers size (Fig. 13C). This loss of function corroborates the conclusion that size determines the hemostatic potential of vWF multimers (Budde et al., 2006; Favaloro and Koutts, 1997;

Furlan, 1996). Multimer formation and protein-protein interactions differ based on the specific hemostatic diseases.

A wide spectrum of vWF diseases arise from deviations in the multimer distribution compared to the standard normal plasma vWF multimer pattern. This spectrum consists of three major categories: type 1 - characterized by partial quantitative deficiency in vWF multimers, type 2 - characterized by qualitative defects in vWF multimers, and type 3 - characterized by total vWF deficiency. Figure 13D depicts the three different spectrums: vWF disease 1 (sm), 2A (IIC), and 2A (IID). Whereas 1 (sm) and 2A (IID) show a smeared pattern, the 2A (IIC) show an altered pattern of multimers compared to that found in normal plasma. Only a schematic representation of multimers and a severely limited number of vWF diseases are presented here. Our goal is to depict an analogy between vWF and cochlin multimerization in response to shear stress or mechanical stretching. Detailed descriptions of multimer variants and disease association can be found elsewhere (Stockschlaeder et al., 2014).

7.7 Integrating mechanotransduction into AH outflow models

Mechanosensing is a key feature of fluid flow regulation for various conditions in different tissues, such as the kidneys and systemic vasculature. Mechanosensing and mechanotransducing molecules are present in the TM, despite being a very low fluid flow tissue (Goel et al., 2010; Goel et al., 2011; Goel et al., 2012; Tran et al., 2014). The TM mechanosensing axis involves two parts - mechanosensing in the solution phase in the extracellular matrix (ECM) such as with cochlin (Goel et al., 2012) and mechanotransduction on the TM cell surface by various channels (Tran et al., 2014).

Mechanosensing works together with mechanotransduction to initiate various responses. Aberrant mechanosensing can increased resistance at the TM level (Goel et al., 2012). The activity of the TM mechanosensitive channel (Grant et al., 2013) and its modulation regulate cell shape and motility leading to AH outflow regulation (Goel et al., 2011; Goel et al., 2012). Cochlin interacts with Annexin A2 (Goel et al., 2011), SLC44A2 (Kommareddi et al., 2007), and potentially TREK-1 (Goel et al., 2011).

The mechanosensitive channel TREK-1 could underlie cochlin mechanosensing (Goel et al., 2011). However, whether the interaction is direct or indirect and the conditions and domains of these interactions in cochlin remain unknown. We identified ADAMTS2 and ADAMTS4 as potential components in the cleavage of cochlin multimers (Table 1), similar to ADAMTS13 cleavage of vWF (Fig. 13D). Future detailed analyses of multimer quality, degree of multimerization, specific protein interaction, and biological consequences of interaction will provide new insights in this area.

Different mechanosensing and regulatory mechanisms of fluid flow occur in various fluid flow regimes. The kidneys are a leading example of these mechanisms, since mechanotransduction links transcriptional regulation to environmental shear stress or different fluid flow regimes. Fluid flow in the kidneys activates an integral membrane protein polycystin-1 (PC1) (Fig. 13E) (Low et al., 2006).

PC1 generates a truncated part upon flow cessation, which enables the entry of the degraded PC1 fragment into the cells and into the nucleus to stimulate transcriptional regulation of cytoskeletal behavior as well as other cellular dynamics (Fig. 13F). PC1 in the kidneys is an example of a shear sensing mechanism that links external cellular environmental changes (shear stress, mechanical stretching, distortion of tissue or cells) with nuclear transcriptional regulation (Fig. 13E, F).

The PC1 system highlights the complexity associated with ECM changes in different fluid flow regimes and ECM involvement in a complex flow-regulating network. Such transcriptional regulation is unidentified in the TM; however, the existence of such a regulatory arrangement in the TM remains a viable possibility that warrants further exploration.

7.8 Implications of the shared SC vascular and lymphatic characteristics

Vascular and lympatic defects can cause ocular hypertension (Thomson et al., 2014). The inner wall endothelium of SC is the first endothelial-lined conduit or vessel the AH encounters in normal eyes. The molecular composition of SC remained largely uncharacterized until recently. Although SC can express a number of specific vessel and lymphatic markers such as Prox-1, SC is distinguishable from typical lymphatic vessels, since it lacks the lymphatic vessel marker endothelial hyaluronan receptor (LYVE-1) (Truong et al., 2014; van der Merwe and Kidson, 2014). The sprouting reaction due to inflammatory lymphangiogenesis expressed in other regions of ocular tissues such as the cornea is also absent in the SC (Truong et al., 2014).

Developmental studies revealed that the SC is a unique vessel expressing markers for both blood and lymph vessels (Kizhatil et al., 2014). Studies using OCT in perfused and living eyes (Kagemann et al., 2010; Kagemann et al., 2012) and three dimensional mico-computed tomography (3D-micro-CT) (Hann et al., 2011; Hann et al., 2014) now suggest anatomical changes in SC and collector channels occur together in glaucoma.

These findings prompt the following questions. Is the entirety of the TM, the unique composition of SC walls and the distal CC walls a continuum designed to control outflow homeostasis and IOP? Do persistent aberrations and the resultant pathologies in one region have biological consequences that occur distal to other outflow areas? While the TM and SC are undergoing dynamic changes, could the downstream distal collectors also undergo consonant dynamic changes to maintain homeostasis? Future studies will explore these questions to stimulate new insights and develop more targeted therapies (Table 2).

7.9 Distal CCE distribution and flow patterns may underlie segmental TM flow

The vascular anatomy of the distal outflow system partially explains the segmental patterns of aqueous outflow (Hann et al., 2011; Hann and Fautsch, 2009; Hann et al., 2014; Kagemann et al., 2010; Kagemann et al., 2012) (Fig. 2). Aqueous outflow is not uniform but is segmental around the SC circumference. The majority of outflow is likely through the inferior collector channels, particularly in the inferior nasal region (Cha et al., 2016; Grover and Fellman, 2015; Grover et al., 2015; Swaminathan et al., 2014).

Microsphere studies demonstrated the AH flows through the areas of least resistance (Cha et al., 2016; Swaminathan et al., 2013; Swaminathan et al., 2014; Vranka et al., 2015a). Circumferential flow around SC may be limited as AH flow through the TM into SC is diverted into areas where the collector channels are most abundant to create the observed segmental flow pattern. The vascular structures that act as pathways for AH outflow are highly integrated from the proximal TM to the distal ESV. These integrated pathways can explain the dynamic cyclic aqueous flow referred to as “pulsatile flow”. This flow is observed as aqueous discharges from the SC to enter the aqueous veins on the surface of the eye.

8. Surgical insights into outflow system resistance

8.1 Experimental microsurgery: a guide to identify resistance sites

8.1.1 Evidence IOP regulation resides in the AH outflow rather than the inflow system—The discovery of the aqueous veins in the early 1940s (Ascher, 1942) indicated that aqueous flows and IOP control results from a delicate balance between AH inflow and outflow. The work performed by Grant then demonstrated that the primary regulation of IOP resides in the AH outflow system (Grant, 1958). His work also demonstrated that the AH outflow system caused the abnormal pressure elevations in glaucoma (Grant, 1963). These studies provided strong evidence that IOP regulation resides in the AH outflow pathway rather than the inflow pathway. This fundamental advance to understand IOP regulation provides the basic underpinnings for both basic science and the current clinical management of glaucoma (Gabelt and Kaufman, 2011).

Grant’s studies in *ex vivo* human eyes involved removal of the TM, which eliminated about 75% of the resistance in normal eyes (Grant, 1958) and removed the abnormal resistance observed in glaucoma eyes (Grant, 1963). Understandably, evidence from Grant’s work initially indicated that normal IOP control and the abnormal IOP increase found in glaucoma occurred as a result of a problem at the level of the TM. The spaces between the TM lamellae are large compared to the JCT spaces, which are small in unpressurized eyes. This early finding then suggested that outflow resistance was localized to the TM and specifically to the JCT space (Gabelt and Kaufman, 2011).

8..1.2 Experimental microsurgery does not find the TM to be the 1° site of resistance—Most hypotheses regarding AH outflow are based on Grant’s early perfusion studies, so it is useful to examine his more complete later body of work to reveal additional insights involving outflow mechanisms. Grant’s later studies point both to different sites and different resistance mechanisms than those suggested by his early studies (Grant, 1958, 1963). The later studies go far in explaining the limitations of current, minimally invasive glaucoma surgeries (Kaplowitz et al., 2014; Richter and Coleman, 2016).

Grant’s original work did not have histological documentation to determine whether only TM tissue was removed in his microsurgical dissections (Grant, 1958, 1963). Grant and colleagues repeated his studies and found an identical reduction in IOP with TM removal. They reported that during dissections visual inspection indicated that the SC was not a simple tube with binary separation of the inner and outer walls. Instead, these walls had

many connections that prevented experimental isolation of individual walls (Fig. 7). Histologic and scanning electron microscopy studies of the examined tissues further demonstrated the structural elements that attached the two walls of the canal together (Johnstone and Grant, 1973b). Attempts to remove the TM disrupted and damaged structures of the distal pathway along the SC external wall that attach to the TM.

These dissection and histologic findings suggested that the assumptions of Grant's earlier work warranted revision. Rather than a simple tube, the SC lumen and the surrounding walls are highly complex., The earlier studies could not separate outflow resistance into a proximal TM and a distal SC outer wall. These newer studies indicated that a hypothesis of a a simple dichotomy with most resistance limited to the TM did not accurately characterize the TM-distal pathway relationships (Johnstone and Grant, 1973b).

The absence of a simple TM-distal outflow pathway dichotomy was further emphasized by the work of Ellingsen and Grant. They found that removal of the SC external wall led to a ~75% reduction of resistance, similar to the removal of the inner wall. They concluded that it was the relationships between SC walls that caused resistance rather than separate resistances isolated to either proximal TM or distal locations (Ellingsen and Grant, 1972); such an intrepretation was able to reconcile the otherwise inconsistent findings. They reported that pressure-dependent outward movement of TM tissue was directly observable when the restraining external wall was absent following microsurgical unroofing of the SC. They also found that it was impossible to separate the SC walls without disrupting tissues of both the inner and outer walls.

8.2 Operating room surgery as a guide to identify resistance sites

8.2.1 Glaucoma procedures involving the full thickness of the eye wall—

Definitive surgical procedures to treat glaucoma make a fistula that includes the full thickness of the eye wall to let fluid drain into the subconjunctival space under the surface of the eye. The most widely used procedure is the trabeculectomy (Landers et al., 2012). This procedure makes an opening into the eye under a scleral flap, which is then sutured to reduce the risks from too much filtration.

Such procedures completely bypass the normal outflow channels and can achieve pressures approaching episcleral venous pressure levels. However, fistulizing procedures are often fraught with complications (Watson et al., 1990) such as too much flow or scarring that eventually prevents flow. Blinding infections are another issue that develops as a result of this procedure. For these reasons, surgeons have long sought safer procedures that leave the outflow system in place and avoid direct communication between the anterior chamber and subconjunctival space.

8.3 Surgicalprocedures that remove either SC internal or external wall

These partial thickness procedures provide in vivo insights into IOP control mechanisms. SC operations fall into two broad categories: procedures that make an opening either in the SC outer or inner wall. Despite the many approaches available, none regularly attain the goal of an IOP close to the episcleral venous pressure (Francis et al., 2011). The lack of

achievement of the IOP goal emphasizes our incomplete understanding of outflow system resistance sites and mechanisms.

8.4 Opening or removal of the SC external wall

Sinusotomy (Krasnov, 1968) removes the entire scleral wall of the SC. A deep sclerectomy (Sanchez et al., 1996) removes the deep sclera adjacent to SC but leaves a scleral flap over the area of the removed SC external wall. A viscocanalostomy (Stegmann et al., 1999) introduces a viscoelastic into SC after a deep sclerectomy. Canaloplasty (Stegmann et al., 1999) uses a deep sclerectomy to access SC followed by a suture that completely encapsulates the circumference of the canal. The suture is then tied to create circumferential tension on the TM pulling it inwards toward the anterior chamber.

8.5 Opening of the inner wall of SC

Procedures that provide access to the SC by removing the SC internal wall are performed by two approaches - either from within the anterior chamber or through a scleral incision. A goniotomy is a simple incision into the TM from within the anterior chamber (Barkan, 1949). A trabeculotomy is an external approach that uses a deep scleral incision to access SC (Harms and Dannheim, 1970). A probe is then passed along SC and rotated into the anterior chamber. The procedure also provides a slit-like opening into the canal.

Suture trabeculotomy uses either an external (Smith, 1962, 1969) or internal (Grover and Fellman, 2015) approach to pass a suture or cannula around SC that is then pulled inward. The encircling element completely enters SC to create a 360° opening in the TM. The opening permits communication between the anterior chamber and SC. Procedures that either rotate a probe or use an encircling suture to make an opening into SC typically create a slit opening in the TM near Schwalbe’s line that leaves a complete flap of trabecular tissue in place hinged at the scleral spur (Johnstone and Grant, 1973b). A trabectome is a device that causes ablation of the entire TM tissue over a portion of SC circumference, in contrast to goniotomy, probe, or suture trabeculotomy that leave a slit opening in the TM.

8.6 Devices that provide the AH direct access to SC

Stents have been developed in which one end is placed in the anterior chamber and the other is inserted into SC. The devices may be short (Bahler et al., 2012; Samuelson et al., 2011) or may extend a considerable distance along SC (Camras et al., 2012; Pfeiffer et al., 2015) to create a scaffold that bridge the CCE (Johnstone et al., 2014). These outflow system procedures have recently garnered a great deal of interest, because they access the TM and SC through a very small corneal incision which minimizes intraoperative and postoperative complications. Although they do not achieve pressures as low as those that completely bypass the outflow system, they have a favorable risk benefit ratio.

8.7 Insights from provocative tests in the operating room

A review of in vivo provocative tests yields specific insights related to outflow abnormalities. Provocative testing performed in the operating room prior to canaloplasty (Grieshaber et al., 2010b) reduces IOP and causes blood to reflux into SC. A prospective study demonstrated that those with poor blood reflux had a reduced success rate (Grieshaber

et al., 2010a). The inability to reflux blood can predict surgical failure and can reflect abnormalities of the relationship between SC wall or the distal outflow system.

Fellman and Grover found that flow through distal collector channels in the operating room immediately following trabectome surgery was highly variable (Grover et al., 2014; Grover et al., 2015). They reported that some patients had a vigorous fluid wave and/or a wide area of blanching of the aqueous and episcleral veins on the surface of the eye, while other patients exhibited little evidence of a fluid wave. Those with a vigorous fluid wave had a lower postoperative IOP, while patients with minimal flow through their distal collector channels had a higher postoperative IOP; the latter group may be expected to require further glaucoma surgery more often than patients with a marked blanching of their episcleral and conjunctival vessels (Grover et al., 2014; Grover et al., 2015). Labortory evidence suggests that there is damage to distal collector channels in some patients with POAG. The 3D reconstruction of OCT images in perfused enucleated POAG eyes further corroborates these observations (Fig. 14) (Kagemann et al., 2010; Kagemann et al., 2012).

8.8 Research directions suggested by provocative tests

Blood reflux into SC and the episcleral venous fluid wave can be indicative of the collector channel capacity to transport fluid from the SC to the AH. The effects of mechanosensing, biochemical forces, and vascular homeostasis on the downstream collector channels require further research. In addition, wound healing and remodeling in the canal, and perhaps in the collector channels, may occur following trabectome surgery because the surgery IOP-reducing effects diminish over time.

TM removal markedly alters the anatomy and AH flow patterns that will be experienced by the CCE and the deep scleral plexus following trabectome surgery. Abnormal shear stress or mechanical stretching patterns at the CCE and within the deep scleral plexus may explain aberrant wound healing resulting from altered shear forces on the basement membranes thus leading to angiogenesis. Vessel formation has been observed after canal surgery, but the etiology of this neovascularization has not been explored.

A better understanding of shear forces, mechanosensing, basement membrane structures, and vessel formation may provide greater insights into wound healing in and around SC. A reduction in aberrant wound healing after canal surgery would promote lower IOP and improved vision for glaucoma patients. Animal models of glaucoma should complement and expand our understanding in this area. For example, the DBA/2J mouse shows segmental resistance to outflow (Fig. 15A) and dramatic differences in the distribution of lymphatic and vessel markers in the distal outflow regions (Fig. 15B).

8.9 Reduced intraocular pressure following partial thickness procedures

Procedures that remove SC external wall typically achieve IOP levels in the mid-teens (Grieshaber et al., 2015; Lewis et al., 2011). Procedures that remove or bypass the TM at SC internal wall provide similar pressure reductions (Pfeiffer et al., 2015; Samuelson et al., 2011). Since these procedures do reduce pressure to the mid-teens, they indicate that bypassing the tissues of either the SC internal or external wall reduces resistance to AH outflow. However, the procedures do not generally reduce IOP to near episcleral venous

pressure levels as predicted if most resistance is either localized in the TM or in the distal outflow pathways. The inability to achieve pressure levels at near EVP implicates both the TM and distal pathways as important factors in AH outflow regulation (Swaminathan et al., 2014). The findings indicate further study of synergistic relationships between the pathways will be beneficial.

9. Conclusion

Our premise is that the TM, the collector channels, and the distal outflow pathways function as a highly integrated organ system to control AH flow rather than as isolated regions. We hypothesize and discuss here that aberrant mechanosensing of shear stress or mechanical stretching could occur in the TM and that increased resistance at the TM may be only a part of glaucoma pathology. We propose that alterations in soluble mechanosensing molecules and decreased homeostasis in the pathways distal to SC are part of a pathological axis in glaucoma.

Malfunctions in both the TM and distal portions of the organ system may be integral to glaucoma pathology. Increases in TM resistance, reduced collector channel frequency, or dimensions may underlie a continuum that reduces AH outflow. Increasing stiffness with concomitant alterations in motion may involve both the TM and CCE. Each of these factors may act as additional parameters for consideration in the glaucoma pathology continuum (Fig. 16).

Distal outflow system defects contiguous with low flow TM regions may represent the primary source of dysfunction in a subset of patients. Micro CT (Hann et al., 2011; Hann et al., 2014) and OCT studies (Kagemann et al., 2010; Kagemann et al., 2012) suggest these changes. Newly deveoloped OCT imaging approaches should provide novel insights into structural relationships and pressure-dependent responses. A more complete molecular characterization in aging and glaucoma eyes should be able to assess the probability that this hypothesis is correct.

If reduced CC dimensions are involved, targeted efforts to change CC dimensions may represent an additional therapeutic avenue. Aberrant changes in the flow regulation continuum distributed throughout the pathways from the TM to the distal episcleral vessels could reduce AH outflow. If true, we should revisit AH outflow regulation with a focus on vascular homeostasis. Such a focus may trigger the development of additional efficacious intervention strategies.

Mechanosensing and mechanotransduction characterization is an area of intense research with much progress. In addition, the determination of ECM and BM protein stability and global turnover throughout the AH outflow pathways will provide further insights into the molecular mechanisms. The molecules present under different conditions within these structures should permit testable hypotheses and elucidate their physiological and functional roles. These studies should not only stimulate innovative ideas (Table 2), but should also provide insights to permit development of pioneering intervention strategies.

Acknowledgments

This work was partly supported by an unrestricted grant to University of Miami from Research to Prevent Blindness (RPB), NIH grants EY016112 and EY14801, Department of Defense grant W81XWH-15-1-0079. Figure 2 B–E and Figure 9 A & B are courtesy of the Johnstone Glaucoma Laboratory at the University of Washington.

References

Anderson DR. Glaucoma: the damage caused by pressure. XLVI Edward Jackson memorial lecture. Am J Ophthalmol. 1989; 108:485–495. [PubMed: 2683792]

Anderson DR. Collaborative normal tension glaucoma study. Curr Opin Ophthalmol. 2003; 14:86–90. [PubMed: 12698048]

Ascher KW. Physiologic importance of the visible elimination of intraocular fluid. Am J Ophth. 1942; 25:1174–1209.

Ascher KW. Backflow phenomena in aqueous veins. Am J Ophth. 1944; 27:1074–1076.

Ascher KW. Aqueous veins and their significance for pathogenesis of glaucoma. Arch Ophthal. 1949; 42:66–76.

Ascher KW. Aqueous veins; their status eleven years after their detection. Ama Arch Opthalmol. 1953; 49:438–451.

Ascher, KW. The aqueous veins: biomicroscopic study of aqueous humor elimination. Charles C. Thomas; Springfield, Illinois: 1961.

Asher KW. Aqueous Veins. Am J Ophthalmol. 1942; 25:31–38.

Asrani S, Zeimer R, Wilensky J, Gieser D, Vitale S, Lindenmuth K. Large diurnal fluctuations in intraocular pressure are an independent risk factor in patients with glaucoma. J Glaucoma. 2000; 9:134–142. [PubMed: 10782622]

Bahler CK, Hann CR, Fjield T, Haffner D, Heitzmann H, Fautsch MP. Second-generation trabecular meshwork bypass stent (iStent inject) increases outflow facility in cultured human anterior segments. Am J Ophthalmol. 2012; 153:1206–1213. [PubMed: 22464365]

Barkan O. Technic of goniotomy for congenital glaucoma. Arch Ophthal. 1949; 41:65–82.

Bentley MD, Hann CR, Fautsch MP. Anatomical Variation of Human Collector Channel Orifices. Invest Ophthalmol Vis Sci. 2016; 57:1153–1159. [PubMed: 26975026]

Bhattacharya SK. Focus on molecules: cochlin. Exp Eye Res. 2006; 82:355–356. [PubMed: 16297912]

Bhattacharya SK, Annangudi SP, Salomon RG, Kuchtey RW, Peachey NS, Crabb JW. Cochlin deposits in the trabecular meshwork of the glaucomatous DBA/2J mouse. Exp Eye Res. 2005a; 80:741–744. [PubMed: 15862180]

Bhattacharya, SK., Carreon, T. Lack of Basement Membrane Protein Degradation in Glaucomatous Trabecular Meshwork. In: Semba, R.Ueffing, M., Chung, H., editors. EyeOME Workshop, 2015 HUPO Meeting; Vancouver, Canada: HUPO; 2015.

Bhattacharya SK, Peachey NS, Crabb JW. Cochlin and glaucoma: a mini-review. Vis Neurosci. 2005b; 22:605–613. [PubMed: 16332271]

Bhattacharya SK, Rockwood EJ, Smith SD, Bonilha VL, Crabb JS, Kuchtey RW, Robertson NG, Peachey NS, Morton CC, Crabb JW. Proteomics reveals cochlin deposits associated with glaucomatous trabecular meshwork. J Biol Chem. 2005c; 280:6080–6084. [PubMed: 15579465]

Bignon M, Pichol-Thievend C, Hardouin J, Malbouyres M, Brechot N, Nasciutti L, Barret A, Teillon J, Guillon E, Etienne E, Caron M, Joubert-Caron R, Monnot C, Ruggiero F, Muller L, Germain S. Lysyl oxidase-like protein-2 regulates sprouting angiogenesis and type IV collagen assembly in the endothelial basement membrane. Blood. 2011; 118:3979–3989. [PubMed: 21835952]

Bill A. Uveoscleral drainage of aqueous humor: physiology and pharmacology. Prog Clin Biol Res. 1989; 312:417–427. [PubMed: 2678147]

Bill A, Phillips CI. Uveoscleral drainage of aqueous humour in human eyes. Exp Eye Res. 1971; 12:275–281. [PubMed: 5130270]

Bill A, Svedbergh B. Scanning electron microscopic studies of the trabecular meshwork and the canal of Schlemm--an attempt to localize the main resistance to outflow of aqueous humor in man. Acta Ophthalmol (Copenh). 1972; 50:295–320. [PubMed: 4678226]

Braakman ST, Read AT, Chan DW, Ethier CR, Overby DR. Colocalization of outflow segmentation and pores along the inner wall of Schlemm's canal. Exp Eye Res. 2015; 130:87–96. [PubMed: 25450060]

Bradley JM, Kelley MJ, Zhu X, Anderssohn AM, Alexander JP, Acott TS. Effects of mechanical stretching on trabecular matrix metalloproteinases. Invest Ophthalmol Vis Sci. 2001; 42:1505–1513. [PubMed: 11381054]

Budde U, Pieconka A, Will K, Schneppenheim R. Laboratory testing for von Willebrand disease: contribution of multimer analysis to diagnosis and classification. Semin Thromb Hemost. 2006; 32:514–521. [PubMed: 16862525]

Buller C, Johnson D. Segmental variability of the trabecular meshwork in normal and glaucomatous eyes. Invest Ophthalmol Vis Sci. 1994; 35:3841–3851. [PubMed: 7928181]

Bussel II, Wollstein G, Schuman JS. OCT for glaucoma diagnosis, screening and detection of glaucoma progression. Br J Ophthalmol. 2014; 98(Suppl 2):ii15–19. [PubMed: 24357497]

Camras LJ, Yuan F, Fan S, Samuelson TW, Ahmed IK, Schieber AT, Toris CB. A Novel Schlemm's Canal Scaffold Increases Outflow Facility in a Human Anterior Segment Perfusion Model. Invest Ophthalmol Vis Sci. 2012; 53:6115–6121. [PubMed: 22893672]

Candiello J, Cole GJ, Halfter W. Age-dependent changes in the structure, composition and biophysical properties of a human basement membrane. Matrix Biol. 2010; 29:402–410. [PubMed: 20362054]

Cha ED, Xu J, Gong L, Gong H. Variations in active outflow along the trabecular outflow pathway. Exp Eye Res. 2016 In press.

Chang JY, Folz SJ, Laryea SN, Overby DR. Multi-scale analysis of segmental outflow patterns in human trabecular meshwork with changing intraocular pressure. J Ocul Pharmacol Ther. 2014; 30:213–223. [PubMed: 24456518]

Civan MM, Macknight AD. The ins and outs of aqueous humour secretion. Exp Eye Res. 2004; 78:625–631. [PubMed: 15106942]

Clark ER, Clark EL. Microscopic observation on the growth of blood capillaries in the living organisms. Am J Anat. 1938; 64:251–264.

Coleman AL. Glaucoma. Lancet. 1999; 354:1803–1810. [PubMed: 10577657]

Coleman, AL. Epidemiology of Glaucoma. In: Morrison, JC., Pollack, IP., editors. Glaucoma Science and Practice. Thieme Medical Publishers Inc; New York: 2003. p. 2-11.

de Kater AW, Shahsafaei A, Epstein DL. Localization of smooth muscle and nonmuscle actin isoforms in the human aqueous outflow pathway. Invest Ophthalmol Vis Sci. 1992; 33:424–429. [PubMed: 1740375]

de Kater AW, Spurr-Michaud SJ, Gipson IK. Localization of smooth muscle myosin-containing cells in the aqueous outflow pathway. Invest Ophthalmol Vis Sci. 1990; 31:347–353. [PubMed: 2406217]

Deng Q, Huo Y, Luo J. Endothelial mechanosensors: the gatekeepers of vascular homeostasis and adaptation under mechanical stress. Sci China Life Sci. 2014; 57:755–762. [PubMed: 25104447]

Dvorak-Theobald G, Kirk HQ. Aqueous pathways in some cases of glaucoma. Trans Am Ophthalmol Soc. 1955; 53:301–315. discussion, 315–309. [PubMed: 13360882]

Ellingsen BA, Grant WM. The relationship of pressure and aqueous outflow in enucleated human eyes. Invest Ophthalmol. 1971; 10:430–437. [PubMed: 5578207]

Ellingsen BA, Grant WM. Trabeculotomy and sinusotomy in enucleated human eyes. Invest Ophthalmol. 1972; 11:21–28. [PubMed: 5006959]

Ethier, CR. Estimates of Trabecular Meshwork Stiffness Using Novel Approaches. XXII Biennial Meeting of the Interantional Society for Eye Research; Tokyo, Japan. 2016.

Favaloro EJ, Koutts J. Laboratory assays for von Willebrand factor: relative contribution to the diagnosis of von Willebrand's disease. Pathology. 1997; 29:385–391. [PubMed: 9423220]

Fercher AF, Drexler W, Hitzenberger CK, Lasser T. Optical coherence tomography-principles and applications. Reports on progress in physics. 2003; 66:239–303.

Folkman J, D'Amore PA. Blood vessel formation: what is its molecular basis? Cell. 1996; 87:1153–1155. [PubMed: 8980221]

Form DM, Pratt BM, Madri JA. Endothelial cell proliferation during angiogenesis. In vitro modulation by basement membrane components. Lab Invest. 1986; 55:521–530. [PubMed: 2430138]

Francis BA, Singh K, Lin SC, Hodapp E, Jampel HD, Samples JR, Smith SD. Novel glaucoma procedures: a report by the American Academy of Ophthalmology. Ophthalmology. 2011; 118:1466–1480. [PubMed: 21724045]

Freddo TF. The Glenn A. Fry Award Lecture 1992: aqueous humor proteins: a key for unlocking glaucoma? Optom Vis Sci. 1993; 70:263–270. [PubMed: 8502454]

Friberg TR, Sanborn G, Weinreb RN. Intraocular and episcleral venous pressure increase during inverted posture. Am J Ophthalmol. 1987; 103:523–526. [PubMed: 3565513]

Friberg TR, Weinreb RN. Ocular manifestations of gravity inversion. Jama. 1985; 253:1755–1757. [PubMed: 3974054]

Furlan M. Von Willebrand factor: molecular size and functional activity. Ann Hematol. 1996; 72:341–348. [PubMed: 8767102]

Gabelt, BT., Kaufman, PL. Production and Flow of Aqueous Humor. In: Kaufman, PL., Alm, A., editors. Adler's physiology of the eye. Elsevier; Edinburgh: 2011. p. 274-307.

Goel M, Picciani RG, Lee RK, Bhattacharya SK. Aqueous humor dynamics: a review. Open Ophthalmol J. 2010; 4:52–59. [PubMed: 21293732]

Goel M, Sienkiewicz AE, Picciani R, Lee RK, Bhattacharya SK. Cochlin induced TREK-1 co-expression and annexin A2 secretion: role in trabecular meshwork cell elongation and motility. PLoS One. 2011; 6:e23070. [PubMed: 21886777]

Goel M, Sienkiewicz AE, Picciani R, Wang J, Lee RK, Bhattacharya SK. Cochlin, intraocular pressure regulation and mechanosensing. PLoS One. 2012; 7:e34309. [PubMed: 22496787]

Goldmann H. Abfluss des Kammerwassers beim Menschen. Ophthalmologica. 1946; 111:146–152. [PubMed: 20275796]

Gonzalez JM Jr, Hamm-Alvarez S, Tan JC. Analyzing live cellularity in the human trabecular meshwork. Invest Ophthalmol Vis Sci. 2013; 54:1039–1047. [PubMed: 23249706]

Gonzalez JM Jr, Hsu HY, Tan JC. Observing live actin in the human trabecular meshwork. Clin Exp Ophthalmol. 2014; 42:502–504. [PubMed: 24304516]

Gonzalez JM, Ko MK, Pouw A, Tan JC. Tissue-based multiphoton analysis of actomyosin and structural responses in human trabecular meshwork. Sci Rep. 2016; 6:21315. [PubMed: 26883567]

Grant J, Tran V, Bhattacharya SK, Bianchi L. Ionic currents of human trabecular meshwork cells from control and glaucoma subjects. J Membr Biol. 2013; 246:167–175. [PubMed: 23135060]

Grant WM. Further studies on facility of flow through the trabecular meshwork. Ama Arch Opthalmol. 1958; 60:523–533.

Grant WM. Experimental aqueous perfusion in enucleated human eyes. Arch Ophthalmol. 1963; 69:783–801. [PubMed: 13949877]

Grierson I, Lee WR. Changes in the monkey outflow apparatus at graded levels of intraocular pressure: a qualitative analysis by light microscopy and scanning electron microscopy. Exp Eye Res. 1974; 19:21–33. [PubMed: 4412389]

Grierson I, Lee WR. The fine structure of the trabecular meshwork at graded levels of intraocular pressure. (1) Pressure effects within the near-physiological range (8–30 mmHg). Exp Eye Res. 1975a; 20:505–521. [PubMed: 1149832]

Grierson I, Lee WR. The fine structure of the trabecular meshwork at graded levels of intraocular pressure. (2) Pressures outside the physiological range (0 and 50 mmHg). Exp Eye Res. 1975b; 20:523–530. [PubMed: 168092]

Grieshaber MC, Peckar C, Pienaar A, Koerber N, Stegmann R. Long-term results of up to 12 years of over 700 cases of viscocanalostomy for open-angle glaucoma. Acta Ophthalmol. 2015; 93:362–367. [PubMed: 25270165]

Grieshaber MC, Pienaar A, Olivier J, Stegmann R. Canaloplasty for primary open-angle glaucoma: long-term outcome. Br J Ophthalmol. 2010a; 94:1478–1482. [PubMed: 20962352]

Grieshaber MC, Pienaar A, Olivier J, Stegmann R. Clinical evaluation of the aqueous outflow system in primary open-angle glaucoma for canaloplasty. Invest Ophthalmol Vis Sci. 2010b; 51:1498–1504. [PubMed: 19933180]

Grover DS, Fellman RL. Gonioscopy-assisted Transluminal Trabeculotomy (GATT): Thermal Suture Modification With a Dye-stained Rounded Tip. J Glaucoma. 2015 In press.

Grover DS, Godfrey DG, Smith O, Feuer WJ, Montes de Oca I, Fellman RL. Gonioscopy-assisted transluminal trabeculotomy, ab interno trabeculotomy: technique report and preliminary results. Ophthalmology. 2014; 121:855–861. [PubMed: 24412282]

Grover DS, Smith O, Fellman RL, Godfrey DG, Butler MR, Montes de Oca I, Feuer WJ. Gonioscopy assisted transluminal trabeculotomy: an ab interno circumferential trabeculotomy for the treatment of primary congenital glaucoma and juvenile open angle glaucoma. Br J Ophthalmol. 2015; 99:1092–1096. [PubMed: 25677669]

Haddadin RI, Oh DJ, Kang MH, Filippopoulos T, Gupta M, Hart L, Sage EH, Rhee DJ. SPARC-null mice exhibit lower intraocular pressures. Invest Ophthalmol Vis Sci. 2009; 50:3771–3777. [PubMed: 19168904]

Haddadin RI, Oh DJ, Kang MH, Villarreal G Jr, Kang JH, Jin R, Gong H, Rhee DJ. Thrombospondin-1 (TSP1)-null and TSP2-null mice exhibit lower intraocular pressures. Invest Ophthalmol Vis Sci. 2012; 53:6708–6717. [PubMed: 22930728]

Halfter W, Oertle P, Monnier CA, Camenzind L, Reyes-Lua M, Hu H, Candiello J, Labilloy A, Balasubramani M, Henrich PB, Plodinec M. New concepts in basement membrane biology. Febs J. 2015; 282:4466–4479. [PubMed: 26299746]

Hann CR, Bentley MD, Vercnocke A, Ritman EL, Fautsch MP. Imaging the aqueous humor outflow pathway in human eyes by three-dimensional microcomputed tomography (3D micro-CT). Exp Eye Res. 2011; 92:104–111. [PubMed: 21187085]

Hann CR, Fautsch MP. Preferential fluid flow in the human trabecular meshwork near collector channels. Invest Ophthalmol Vis Sci. 2009; 50:1692–1697. [PubMed: 19060275]

Hann CR, Springett MJ, Wang X, Johnson DH. Ultrastructural localization of collagen IV, fibronectin, and laminin in the trabecular meshwork of normal and glaucomatous eyes. Ophthalmic Res. 2001; 33:314–324. [PubMed: 11721183]

Hann CR, Vercnocke AJ, Bentley MD, Jorgensen SM, Fautsch MP. Anatomic changes in Schlemm's canal and collector channels in normal and primary open-angle glaucoma eyes using low and high perfusion pressures. Invest Ophthalmol Vis Sci. 2014; 55:5834–5841. [PubMed: 25139736]

Hariri S, Johnstone M, Jiang Y, Padilla S, Zhou Z, Reif R, Wang RK. Platform to investigate aqueous outflow system structure and pressure-dependent motion using high-resolution spectral domain optical coherence tomography. J Biomed Opt. 2014; 19:106013. [PubMed: 25349094]

Harms H, Dannheim R. Trabeculotomy 'ab externo'. Trans Ophthalmol Soc U K. 1970; 89:589–590. [PubMed: 5276690]

Hogan, MJ., Alvarado, J., Weddell, JE. Histology of the human eye, and atlas and textbook. Saunders; Philadelphia: 1971.

Huang D, Swanson EA, Lin CP, Schuman JS, Stinson WG, Chang W, Hee MR, Flotte T, Gregory K, Puliafito CA, et al. Optical coherence tomography. Science. 1991; 254:1178–1181. [PubMed: 1957169]

Johnson M, Shapiro A, Ethier CR, Kamm RD. Modulation of outflow resistance by the pores of the inner wall endothelium. Invest Ophthalmol Vis Sci. 1992; 33:1670–1675. [PubMed: 1559767]

Johnstone, M., Jamil, A., Martin, E. Aqueous Veins and Open Angle Glaucoma. In: Schacknow, P., Samples, JR., editors. The Glaucoma Book. Springer; New York: 2010.

Johnstone M, Martin E, Jamil A. Pulsatile flow into the aqueous veins: manifestations in normal and glaucomatous eyes. Exp Eye Res. 2011; 92:318–327. [PubMed: 21440541]

Johnstone M, Tanner D, Chau B, Kopecky K. Concentration-dependent morphologic effects of cytochalasin B in the aqueous outflow system. Invest Ophthalmol Vis Sci. 1980; 19:835–841. [PubMed: 6771222]

Johnstone MA. Pressure-dependent changes in configuration of the endothelial tubules of Schlemm's canal. Am J Ophthalmol. 1974; 78:630–638. [PubMed: 4415190]

Johnstone MA. The aqueous outflow system as a mechanical pump: evidence from examination of tissue and aqueous movement in human and non-human primates. J Glaucoma. 2004; 13:421–438. [PubMed: 15354083]

Johnstone, MA. Intraocular pressure control through linked trabecular meshwork and collector channel motion. In: Samples, JR., Knepper, PA., editors. Glaucoma Research and Clinical Advances: 2016 to 2018. Kugler Publications; Amsterdam: 2016.

Johnstone MA, Grant WG. Pressure-dependent changes in structures of the aqueous outflow system of human and monkey eyes. Am J Ophthalmol. 1973a; 75:365–383. [PubMed: 4633234]

Johnstone MA, Grant WM. Microsurgery of Schlemm's canal and the human aqueous outflow system. Am J Ophthalmol. 1973b; 76:906–917. [PubMed: 4759850]

Johnstone MA, Saheb H, Ahmed II, Samuelson TW, Schieber AT, Toris CB. Effects of a Schlemm canal scaffold on collector channel ostia in human anterior segments. Exp Eye Res. 2014; 119:70–76. [PubMed: 24374259]

Kagemann L, Wollstein G, Ishikawa H, Bilonick RA, Brennen PM, Folio LS, Gabriele ML, Schuman JS. Identification and assessment of Schlemm's canal by spectral-domain optical coherence tomography. Invest Ophthalmol Vis Sci. 2010; 51:4054–4059. [PubMed: 20237244]

Kagemann L, Wollstein G, Ishikawa H, Nadler Z, Sigal IA, Folio LS, Schuman JS. Visualization of the conventional outflow pathway in the living human eye. Ophthalmology. 2012; 119:1563–1568. [PubMed: 22683063]

Kalluri R. Basement membranes: structure, assembly and role in tumour angiogenesis. Nat Rev Cancer. 2003; 3:422–433. [PubMed: 12778132]

Kaplowitz K, Schuman JS, Loewen NA. Techniques and outcomes of minimally invasive trabecular ablation and bypass surgery. Br J Ophthalmol. 2014; 98:579–585. [PubMed: 24338085]

Keller KE, Aga M, Bradley JM, Kelley MJ, Acott TS. Extracellular matrix turnover and outflow resistance. Exp Eye Res. 2009a; 88:676–682. [PubMed: 19087875]

Keller KE, Bradley JM, Acott TS. Differential effects of ADAMTS-1, -4, and -5 in the trabecular meshwork. Invest Ophthalmol Vis Sci. 2009b; 50:5769–5777. [PubMed: 19553617]

Keller KE, Bradley JM, Kelley MJ, Acott TS. Effects of modifiers of glycosaminoglycan biosynthesis on outflow facility in perfusion culture. Invest Ophthalmol Vis Sci. 2008; 49:2495–2505. [PubMed: 18515587]

Keller KE, Sun YY, Vranka JA, Hayashi L, Acott TS. Inhibition of hyaluronan synthesis reduces versican and fibronectin levels in trabecular meshwork cells. PLoS One. 2012; 7:e48523. [PubMed: 23139787]

Kilarski WW, Samolov B, Petersson L, Kvanta A, Gerwins P. Biomechanical regulation of blood vessel growth during tissue vascularization. Nat Med. 2009; 15:657–664. [PubMed: 19483693]

Kizhatil K, Ryan M, Marchant JK, Henrich S, John SW. Schlemm's canal is a unique vessel with a combination of blood vascular and lymphatic phenotypes that forms by a novel developmental process. PLoS Biol. 2014; 12:e1001912. [PubMed: 25051267]

Kleinert HW. The compensation maximum; a new glaucoma sign in aqueous veins. AMA Arch Ophthalmol. 1951; 46:618–624. [PubMed: 14868091]

Ko MK, Kim EK, Gonzalez JM Jr, Tan JC. Dose- and time-dependent effects of actomyosin inhibition on live mouse outflow resistance and aqueous drainage tissues. Sci Rep. 2016; 6:21492. [PubMed: 26884319]

Kommareddi PK, Nair TS, Raphael Y, Telian SA, Kim AH, Arts HA, El-Kashlan HK, Carey TE. Cochlin isoforms and their interaction with CTL2 (SLC44A2) in the inner ear. J Assoc Res Otolaryngol. 2007; 8:435–446. [PubMed: 17926100]

Krasnov MM. Externalization of Schlemm's canal (sinusotomy) in glaucoma. Br J Ophthalmol. 1968; 52:157–161. [PubMed: 5642665]

Kronfeld PC. Gonioscopic correlates of responsiveness to miotics. Arch Ophthal. 1944; 32:447–455.

Kronfeld PC. Further gonioscopic studies on the canal of Schlemm. Arch Ophthal. 1949; 41:393–405.

Kronfeld PC, McGarry HT, Smith HE. Gonioscopic study on the canal of Schlemm. Am J Ophthal. 1942; 25:1163–1173.

Kuchtey J, Kuchtey RW. The microfibril hypothesis of glaucoma: implications for treatment of elevated intraocular pressure. J Ocul Pharmacol Ther. 2014; 30:170–180. [PubMed: 24521159]

Landers J, Martin K, Sarkies N, Bourne R, Watson P. A twenty-year follow-up study of trabeculectomy: risk factors and outcomes. Ophthalmology. 2012; 119:694–702. [PubMed: 22196977]

Last JA, Pan T, Ding Y, Reilly CM, Keller K, Acott TS, Fautsch MP, Murphy CJ, Russell P. Elastic modulus determination of normal and glaucomatous human trabecular meshwork. Invest Ophthalmol Vis Sci. 2011; 52:2147–2152. [PubMed: 21220561]

Lechene C, Hillion F, McMahon G, Benson D, Kleinfeld AM, Kampf JP, Distel D, Luyten Y, Bonventre J, Hentschel D, Park KM, Ito S, Schwartz M, Benichou G, Slodzian G. High-resolution quantitative imaging of mammalian and bacterial cells using stable isotope mass spectrometry. J Biol. 2006; 5:20. [PubMed: 17010211]

Lee WR, Grierson I. Relationships between intraocular pressure and the morphology of the outflow apparatus. Trans Ophthalmol Soc U K. 1974; 94:430–449. [PubMed: 4219862]

Levick, JR. Introduction to Cardiovascular Physiology. Hodder Education, a Hachette UK Company; London: 2010.

Lewis RA, von Wolff K, Tetz M, Koerber N, Kearney JR, Shingleton BJ, Samuelson TW. Canaloplasty: Three-year results of circumferential viscodilation and tensioning of Schlemm canal using a microcatheter to treat open-angle glaucoma. J Cataract Refract Surg. 2011; 37:682–690. [PubMed: 21420593]

Loewen NA, Schuman JS. There has to be a better way: evolution of internal filtration glaucoma surgeries. Br J Ophthalmol. 2013; 97:1228–1229. [PubMed: 24049122]

Low SH, Vasanth S, Larson CH, Mukherjee S, Sharma N, Kinter MT, Kane ME, Obara T, Weimbs T. Polycystin-1, STAT6, and P100 function in a pathway that transduces ciliary mechanosensation and is activated in polycystic kidney disease. Dev Cell. 2006; 10:57–69. [PubMed: 16399078]

Lutjen-Drecoll E. Electron microscopic studies on reactive changes of the trabecular meshwork in human eyes after microsurgery. Albrecht Von Graefes Arch Klin Exp Ophthalmol. 1972; 183:267–285. [PubMed: 4111809]

Lutjen-Drecoll E. New findings on the functional structure of the region of the angle of the chamber and its changes after glaucoma surgery (author's transl). Klin Monatsbl Augenheilkd. 1973; 163:410–419. [PubMed: 4204610]

Lutjen-Drecoll E. Functional morphology of the trabecular meshwork in primate eyes. Prog Retin Eye Res. 1999; 18:91–119. [PubMed: 9920500]

Lutjen-Drecoll E. Importance of trabecular meshwork changes in the pathogenesis of primary open-angle glaucoma. J Glaucoma. 2000; 9:417–418. [PubMed: 11131746]

Lutjen-Drecoll E, Barany EH. Functional and electron microscopic changes in the trabecular meshwork remaining after trabeculectomy in cynomolgus monkeys. Invest Ophthalmol. 1974; 13:511–524. [PubMed: 4209932]

Lutjen-Drecoll E, Draeger J, Rohen JW. Histological examination on structural changes in the region of the angle of the anterior chamber after microsurgical glaucoma operations. Klin Monatsbl Augenheilkd. 1972; 160:281–292. [PubMed: 4554468]

Lutjen-Drecoll E, Eichhorn M. Morphological principles of the aqueous humor secretory system and its changes induced by antiglaucoma drugs. Fortschr Ophthalmol. 1988; 85:25–32. [PubMed: 3371812]

Lutjen-Drecoll E, Futa R, Rohen JW. Ultrahistochemical studies on tangential sections of the trabecular meshwork in normal and glaucomatous eyes. Invest Ophthalmol Vis Sci. 1981; 21:563–573. [PubMed: 7287346]

Lutjen-Drecoll E, Shimizu T, Rohrbach M, Rohen JW. Quantitative analysis of 'plaque material' between ciliary muscle tips in normal- and glaucomatous eyes. Exp Eye Res. 1986; 42:457–465. [PubMed: 3720864]

Madri JA. Extracellular matrix modulation of vascular cell behaviour. Transpl Immunol. 1997; 5:179–183. [PubMed: 9402683]

Mao M, Hedberg-Buenz A, Koehn D, John SW, Anderson MG. Anterior segment dysgenesis and early-onset glaucoma in nee mice with mutation of Sh3pxd2b. Invest Ophthalmol Vis Sci. 2011; 52:2679–2688. [PubMed: 21282566]

Moake JL, Turner NA, Stathopoulos NA, Nolasco LH, Hellums JD. Involvement of large plasma von Willebrand factor (vWF) multimers and unusually large vWF forms derived from endothelial cells in shear stress-induced platelet aggregation. J Clin Invest. 1986; 78:1456–1461. [PubMed: 3491092]

Morgan JT, Raghunathan VK, Chang YR, Murphy CJ, Russell P. Wnt inhibition induces persistent increases in intrinsic stiffness of human trabecular meshwork cells. Exp Eye Res. 2015; 132:174–178. [PubMed: 25639201]

Morrison, JC., Acott, TS. Anatomy and physiology of aqueous humor outflow. In: Morrison, JC., Pollack, IP., editors. Glaucoma Science and Practice. Thieme Medical Publishers Inc; New York: 2003. p. 34-41.

Overby DR, Bertrand J, Tektas OY, Boussommier-Calleja A, Schicht M, Ethier CR, Woodward DF, Stamer WD, Lutjen-Drecoll E. Ultrastructural changes associated with dexamethasone-induced ocular hypertension in mice. Invest Ophthalmol Vis Sci. 2014; 55:4922–4933. [PubMed: 25028360]

Park DY, Lee J, Park I, Choi D, Lee S, Song S, Hwang Y, Hong KY, Nakaoka Y, Makinen T, Kim P, Alitalo K, Hong YK, Koh GY. Lymphatic regulator PROX1 determines Schlemm's canal integrity and identity. J Clin Invest. 2014a; 124:3960–3974. [PubMed: 25061877]

Park HY, Kim JH, Park CK. Lysyl oxidase-like 2 level and glaucoma surgical outcomes. Invest Ophthalmol Vis Sci. 2014b; 55:3337–3343. [PubMed: 24764069]

Patel N, Solanki E, Picciani R, Cavett V, Caldwell-Busby JA, Bhattacharya SK. Strategies to recover proteins from ocular tissues for proteomics. Proteomics. 2008; 8:1055–1070. [PubMed: 18324731]

Perez-Silva JG, Espanol Y, Velasco G, Quesada V. The Degradome database: expanding roles of mammalian proteases in life and disease. Nucleic Acids Res. 2016; 44:D351–355. [PubMed: 26553809]

Pfeiffer N, Garcia-Feijoo J, Martinez-de-la-Casa JM, Larrosa JM, Fea A, Lemij H, Gandolfi S, Schwenn O, Lorenz K, Samuelson TW. A Randomized Trial of a Schlemm's Canal Microstent with Phacoemulsification for Reducing Intraocular Pressure in Open-Angle Glaucoma. Ophthalmology. 2015; 122:1283–1293. [PubMed: 25972254]

Phillips CI, Tsukahara S, Hosaka O, Adams W. Ocular pulsation correlates with ocular tension: the choroid as piston for an aqueous pump? Ophthalmic Res. 1992; 24:338–343. [PubMed: 1287513]

Picciani R, Desai K, Guduric-Fuchs J, Cogliati T, Morton CC, Bhattacharya SK. Cochlin in the eye: functional implications. Prog Retin Eye Res. 2007a; 26:453–469. [PubMed: 17662637]

Picciani R, Garcia C, Desai K, Guduric-Fuchs J, Cogliati T, Bhattacharya SK. Extracellular Matrix Remodeling in the Glaucomatous Trabecular Meshwork. Invest Ophthalmol Vis Sci. 2007b; 48 E-Abstract 2077.

Prockop DJ, Kivirikko KI. Collagens: molecular biology, diseases, and potentials for therapy. Annu Rev Biochem. 1995; 64:403–434. [PubMed: 7574488]

Quick CM, Ngo BL, Venugopal AM, Stewart RH. Lymphatic pump-conduit duality: contraction of postnodal lymphatic vessels inhibits passive flow. Am J Physiol Heart Circ Physiol. 2009; 296:H662–668. [PubMed: 19122167]

Quick CM, Venugopal AM, Gashev AA, Zawieja DC, Stewart RH. Intrinsic pump-conduit behavior of lymphangions. Am J Physiol Regul Integr Comp Physiol. 2007; 292:R1510–1518. [PubMed: 17122333]

Quigley HA, Broman AT. The number of people with glaucoma worldwide in 2010 and 2020. Br J Ophthalmol. 2006; 90:262–267. [PubMed: 16488940]

Richter GM, Coleman AL. Minimally invasive glaucoma surgery: current status and future prospects. Clin Ophthalmol. 2016; 10:189–206. [PubMed: 26869753]

Robertson NG, Hamaker SA, Patriub V, Aster JC, Morton CC. Subcellular localisation, secretion, and post-translational processing of normal cochlin, and of mutants causing the sensorineural deafness and vestibular disorder, DFNA9. J Med Genet. 2003; 40:479–486. [PubMed: 12843317]

Rohen JW, Lutjen-Drecoll E, Flugel C, Meyer M, Grierson I. Ultrastructure of the trabecular meshwork in untreated cases of primary open-angle glaucoma (POAG). Exp Eye Res. 1993; 56:683–692. [PubMed: 8595810]

Rohen JW, Ogilvie A, Lutjen-Drecoll E. Histoautoradiographic and electron microscopic studies on short-term explant cultures of the glaucomatous trabecular meshwork. Graefes Arch Clin Exp Ophthalmol. 1985; 223:1–8. [PubMed: 3996925]

Rohen JW, Rentsch FJ. Morphology of Schlemm's canal and related vessels in the human eye. Albrecht Von Graefes Arch Klin Exp Ophthalmol. 1968; 176:309–329. [PubMed: 5305008]

Rosenquist R, Epstein D, Melamed S, Johnson M, Grant WM. Outflow resistance of enucleated human eyes at two different perfusion pressures and different extents of trabeculotomy. Curr Eye Res. 1989; 8:1233–1240. [PubMed: 2627793]

Russell P, Johnson M. Elastic modulus determination of normal and glaucomatous human trabecular meshwork. Invest Ophthalmol Vis Sci. 2012; 53:117.

Samuelson TW, Katz LJ, Wells JM, Duh YJ, Giamporcaro JE. Randomized evaluation of the trabecular micro-bypass stent with phacoemulsification in patients with glaucoma and cataract. Ophthalmology. 2011; 118:459–467. [PubMed: 20828829]

Sanchez E, Schnyder CC, Sickenberg M, Chiou AG, Hediguer SE, Mermoud A. Deep sclerectomy: results with and without collagen implant. Int Ophthalmol. 1996; 20:157–162. [PubMed: 9112181]

Savage B, Saldivar E, Ruggeri ZM. Initiation of platelet adhesion by arrest onto fibrinogen or translocation on von Willebrand factor. Cell. 1996; 84:289–297. [PubMed: 8565074]

Savage B, Sixma JJ, Ruggeri ZM. Functional self-association of von Willebrand factor during platelet adhesion under flow. Proc Natl Acad Sci U S A. 2002; 99:425–430. [PubMed: 11756664]

Savas JN, Toyama BH, Xu T, Yates JR 3rd, Hetzer MW. Extremely long-lived nuclear pore proteins in the rat brain. Science. 2012; 335:942. [PubMed: 22300851]

Schirmer KE. Reflux of blood in the canal of Schlemm, quantitated. Can J Ophthalmol. 1969; 4:40–44. [PubMed: 5766336]

Schirmer KE. Gonioscopic assessment of blood in Schlemm's canal. Correlation with glaucoma tests. Arch Ophthalmol. 1971; 85:263–267. [PubMed: 5542862]

Schneider SW, Nuschele S, Wixforth A, Gorzelanny C, Alexander-Katz A, Netz RR, Schneider MF. Shear-induced unfolding triggers adhesion of von Willebrand factor fibers. Proc Natl Acad Sci U S A. 2007; 104:7899–7903. [PubMed: 17470810]

Schuman JS. Spectral domain optical coherence tomography for glaucoma (an AOS thesis). Trans Am Ophthalmol Soc. 2008; 106:426–458. [PubMed: 19277249]

Schuman JS, Chang W, Wang N, de Kater AW, Allingham RR. Excimer laser effects on outflow facility and outflow pathway morphology. Invest Ophthalmol Vis Sci. 1999; 40:1676–1680. [PubMed: 10393035]

Shankaran H, Alexandridis P, Neelamegham S. Aspects of hydrodynamic shear regulating shear-induced platelet activation and self-association of von Willebrand factor in suspension. Blood. 2003; 101:2637–2645. [PubMed: 12456504]

Shankaran H, Neelamegham S. Hydrodynamic forces applied on intercellular bonds, soluble molecules, and cell-surface receptors. Biophys J. 2004; 86:576–588. [PubMed: 14695302]

Shim K, Anderson PJ, Tuley EA, Wiswall E, Sadler JE. Platelet-VWF complexes are preferred substrates of ADAMTS13 under fluid shear stress. Blood. 2008; 111:651–657. [PubMed: 17901248]

Siedlecki CA, Lestini BJ, Kottke-Marchant KK, Eppell SJ, Wilson DL, Marchant RE. Shear-dependent changes in the three-dimensional structure of human von Willebrand factor. Blood. 1996; 88:2939–2950. [PubMed: 8874190]

Sienkiewicz AE, Rosenberg BN, Edwards G, Carreon TA, Bhattacharya SK. Aberrant glycosylation in the human trabecular meshwork. Proteomics Clin Appl. 2014; 8:130–142. [PubMed: 24458570]

Sit AJ, Coloma FM, Ethier CR, Johnson M. Factors affecting the pores of the inner wall endothelium of Schlemm's canal. Invest Ophthalmol Vis Sci. 1997; 38:1517–1525. [PubMed: 9224279]

Skipwith CG, Cao W, Zheng XL. Factor VIII and platelets synergistically accelerate cleavage of von Willebrand factor by ADAMTS13 under fluid shear stress. J Biol Chem. 2010; 285:28596–28603. [PubMed: 20605782]

Smith R. Blood in the canal of Schlemm. Br J Ophthalmol. 1956; 40:358–365. [PubMed: 13355941]

Smith R. Nylon filament trabeculotomy in glaucoma. Trans Ophthalmol Soc U K. 1962; 82:439–454. [PubMed: 13989547]

Smith R. Nylon filament trabeculotomy. Comparison with the results of conventional drainage operations in glaucoma simplex. Trans Ophthalmol Soc N Z. 1969; 21:15–26. [PubMed: 5259088]

Sporn LA, Marder VJ, Wagner DD. von Willebrand factor released from Weibel-Palade bodies binds more avidly to extracellular matrix than that secreted constitutively. Blood. 1987; 69:1531–1534. [PubMed: 3105624]

Stambaugh JL, Fuhs JC, Ascher KW. Study of the compensation-maximum test on aqueous veins. AMA Arch Ophthalmol. 1954; 51:24–31. [PubMed: 13103882]

Stamer WD, Acott TS. Current understanding of conventional outflow dysfunction in glaucoma. Curr Opin Ophthalmol. 2012; 23:135–143. [PubMed: 22262082]

Stegmann R, Pienaar A, Miller D. Viscocanalostomy for open-angle glaucoma in black African patients. J Cataract Refract Surg. 1999; 25:316–322. [PubMed: 10079435]

Stockschlaeder M, Schneppenheim R, Budde U. Update on von Willebrand factor multimers: focus on high-molecular-weight multimers and their role in hemostasis. Blood Coagul Fibrinolysis. 2014; 25:206–216. [PubMed: 24448155]

Suson EB, Schultz RO. Blood in schlemm's canal in glaucoma suspects. A study of the relationship between blood-filling pattern and outflow facility in ocular hypertension. Arch Ophthalmol. 1969; 81:808–812. [PubMed: 5783752]

Swaminathan SS, Oh DJ, Kang MH, Ren R, Jin R, Gong H, Rhee DJ. Secreted protein acidic and rich in cysteine (SPARC)-null mice exhibit more uniform outflow. Invest Ophthalmol Vis Sci. 2013; 54:2035–2047. [PubMed: 23422826]

Swaminathan SS, Oh DJ, Kang MH, Rhee DJ. Aqueous outflow: segmental and distal flow. J Cataract Refract Surg. 2014; 40:1263–1272. [PubMed: 25088623]

Tektas OY, Lutjen-Drecoll E. Structural changes of the trabecular meshwork in different kinds of glaucoma. Exp Eye Res. 2009; 88:769–775. [PubMed: 19114037]

Thomson BR, Heinen S, Jeansson M, Ghosh AK, Fatima A, Sung HK, Onay T, Chen H, Yamaguchi S, Economides AN, Flenniken A, Gale NW, Hong YK, Fawzi A, Liu X, Kume T, Quaggin SE. A lymphatic defect causes ocular hypertension and glaucoma in mice. J Clin Invest. 2014; 124:4320–4324. [PubMed: 25202984]

Thorleifsson G, Magnusson KP, Sulem P, Walters GB, Gudbjartsson DF, Stefansson H, Jonsson T, Jonasdottir A, Jonasdottir A, Stefansdottir G, Masson G, Hardarson GA, Petursson H, Arnarsson A, Motallebipour M, Wallerman O, Wadelius C, Gulcher JR, Thorsteinsdottir U, Kong A, Jonasson F, Stefansson K. Common sequence variants in the LOXL1 gene confer susceptibility to exfoliation glaucoma. Science. 2007; 317:1397–1400. [PubMed: 17690259]

Toyama BH, Savas JN, Park SK, Harris MS, Ingolia NT, Yates JR 3rd, Hetzer MW. Identification of long-lived proteins reveals exceptional stability of essential cellular structures. Cell. 2013; 154:971–982. [PubMed: 23993091]

Tran VT, Ho PT, Cabrera L, Torres JE, Bhattacharya SK. Mechanotransduction channels of the trabecular meshwork. Curr Eye Res. 2014; 39:291–303. [PubMed: 24215462]

Truong TN, Li H, Hong YK, Chen L. Novel characterization and live imaging of Schlemm's canal expressing Prox-1. PLoS One. 2014; 9:e98245. [PubMed: 24827370]

Uechi G, Sun Z, Schreiber EM, Halfter W, Balasubramani M. Proteomic View of Basement Membranes from Human Retinal Blood Vessels, Inner Limiting Membranes, and Lens Capsules. J Proteome Res. 2014

Van Bergen T, Marshall D, Van de Veire S, Vandewalle E, Moons L, Herman J, Smith V, Stalmans I. The role of LOX and LOXL2 in scar formation after glaucoma surgery. Invest Ophthalmol Vis Sci. 2013; 54:5788–5796. [PubMed: 23821193]

Van Buskirk EM. Changes in the facility of aqueous outflow induced by lens depression and intraocular pressure in excised human eyes. Am J Ophthalmol. 1976; 82:736–740. [PubMed: 998694]

Van Buskirk EM, Grant WM. Lens depression and aqueous outflow in enucleated primate eyes. Am J Ophthalmol. 1973; 76:632–640. [PubMed: 4201217]

van der Merwe EL, Kidson SH. The three-dimensional organisation of the post-trabecular aqueous outflow pathway and limbal vasculature in the mouse. Exp Eye Res. 2014; 125:226–235. [PubMed: 24979218]

Vranka JA, Bradley JM, Yang YF, Keller KE, Acott TS. Mapping molecular differences and extracellular matrix gene expression in segmental outflow pathways of the human ocular trabecular meshwork. PLoS One. 2015a; 10:e0122483. [PubMed: 25826404]

Vranka JA, Kelley MJ, Acott TS, Keller KE. Extracellular matrix in the trabecular meshwork: intraocular pressure regulation and dysregulation in glaucoma. Exp Eye Res. 2015b; 133:112–125. [PubMed: 25819459]

Wang H, Edwards G, Garzon C, Piqueras C, Bhattacharya SK. Aqueous humor phospholipids of DBA/2J and DBA/2J-Gpnmb(+)/SjJ mice. Biochimie. 2015; 113:59–68. [PubMed: 25843665]

Warren CM, Iruela-Arispe ML. Podosome rosettes precede vascular sprouts in tumour angiogenesis. Nat Cell Biol. 2014; 16:928–930. [PubMed: 25271481]

Watson PG, Jakeman C, Ozturk M, Barnett MF, Barnett F, Khaw KT. The complications of trabeculectomy (a 20-year follow-up). Eye (Lond). 1990; 4(Pt 3):425–438. [PubMed: 2209905]

Weinreb RN, Cook J, Friberg TR. Effect of inverted body position on intraocular pressure. Am J Ophthalmol. 1984; 98:784–787. [PubMed: 6507552]

Xin C, Johnstone M, Wang N, Wang RK. OCT Study of Mechanical Properties Associated with Trabecular Meshwork and Collector Channel Motion in Human Eyes. PLoS One. 2016a; 11:e0162048. [PubMed: 27598990]

Xin C, Wang RK, Song S, Shen T, Wen J, Martin E, Jiang Y, Padilla S, Johnstone M. Aqueous outflow regulation: Optical coherence tomography implicates pressure-dependent tissue motion. Exp Eye Res. 2016b

Xu J, Rodriguez D, Petitclerc E, Kim JJ, Hangai M, Moon YS, Davis GE, Brooks PC. Proteolytic exposure of a cryptic site within collagen type IV is required for angiogenesis and tumor growth in vivo. J Cell Biol. 2001; 154:1069–1079. [PubMed: 11535623]

Zamir, M., Ritman, E. The Physics of Pulsatile Flow. Springer; New York: 2000.

Zhang DS, Piazza V, Perrin BJ, Rzadzinska AK, Poczatek JC, Wang M, Prosser HM, Ervasti JM, Corey DP, Lechene CP. Multi-isotope imaging mass spectrometry reveals slow protein turnover in hair-cell stereocilia. Nature. 2012; 481:520–524. [PubMed: 22246323]

Zhu JY, Ye W, Wang T, Gong HY. Reversible changes in aqueous outflow facility, hydrodynamics, and morphology following acute intraocular pressure variation in bovine eyes. Chin Med J (Engl). 2013; 126:1451–1457. [PubMed: 23595376]

Highlights

- Elevated intraocular pressure, a characteristic of glaucoma, arises from impaired aqueous humor (AH) outflow.
- The molecular mechanisms responsible for maintaining homeostasis in the conventional outflow pathway is not well understood.
- Mechanistic possibilities assist in explaining the continuum of AH outflow control originating in the trabecular meshwork and extending through collector channels into the episcleral veins.

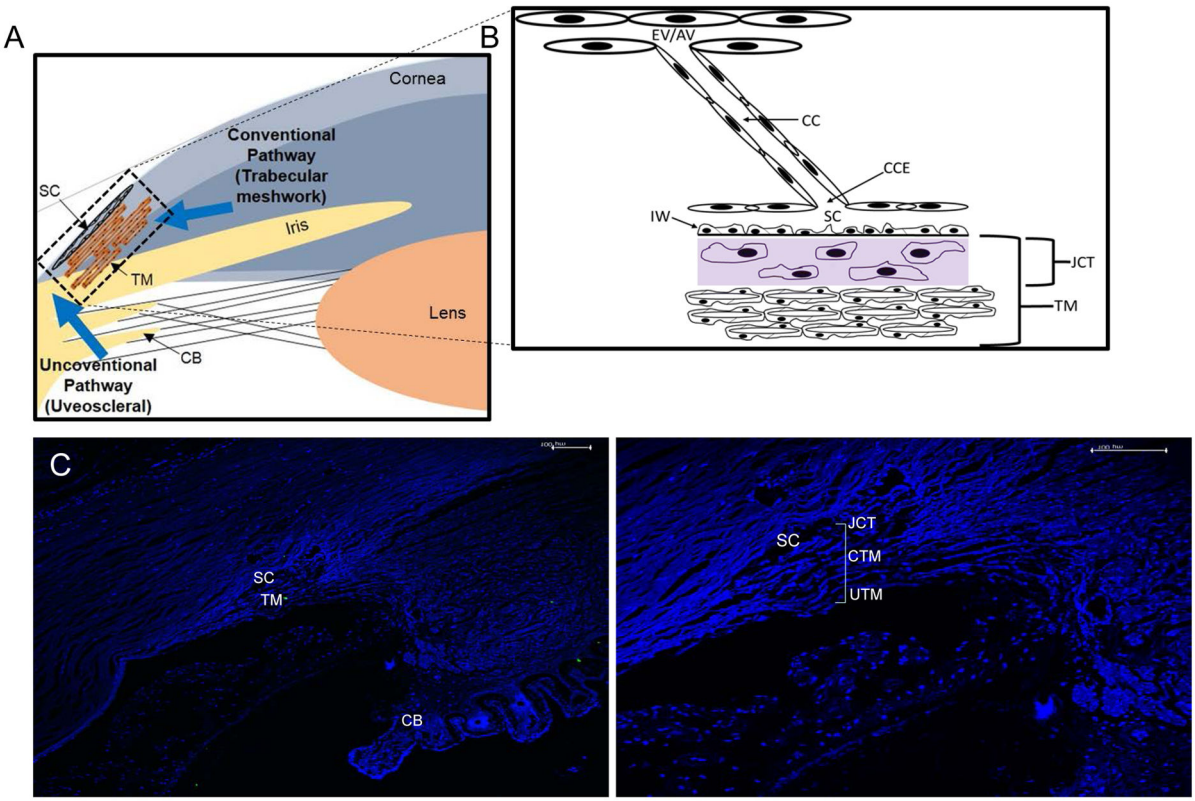

Fig. 1.

Schematic diagram of outflow pathway and structures in the Trabecular Meshwork. **(A)** Schematic diagram depicting conventional and uveoscleral pathway in the anterior eye chamber. **(B)** A magnified view of trabecular meshwork (TM) depicting distal regions including collector channel entrances (CCE), collector channels (CC), episcleral vein (EV), and aqueous vein (AV). **(C)** A DAPI stained image of anterior chamber section showing ciliary body (CB), Schlemm's canal (SC), TM **(D)** A magnified view of the same TM as in C, juxtacanalicular tissue (JCT), uveoscleral (UTM) and conventional (CTM) part of TM is as indicated.

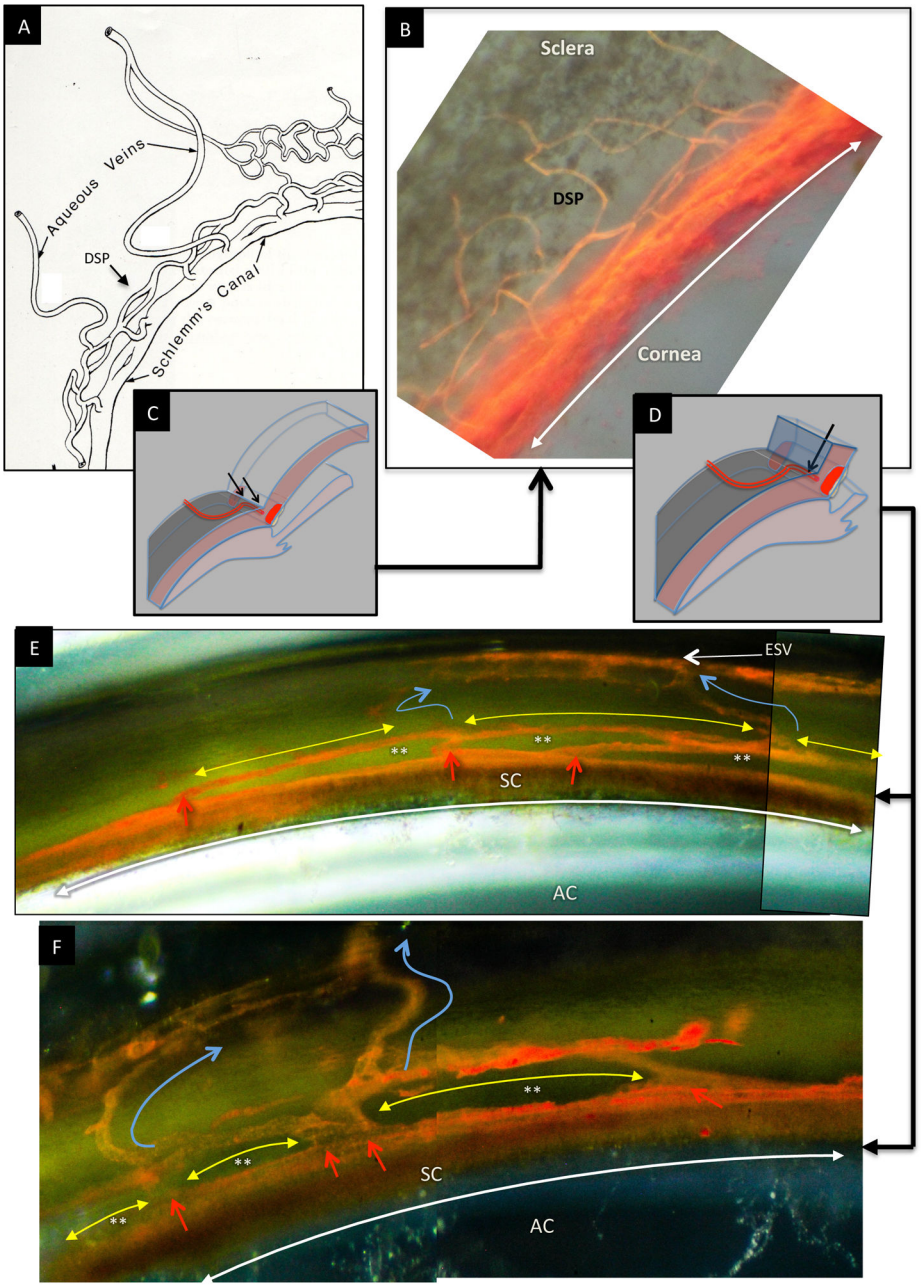

Fig. 2.

Schematic diagram depicting anterior chamber regions **(A)** illustrating the relationship between Schlemm's canal (SC), collector channel entrances (CCE) the deep intrascleral plexus (DSP) and the aqueous veins. **(B)** Microvascular cast of SC, the CCE, the (DSP) and aqueous veins that parallels the appearance of the schematic diagram in (A.) **(C)** Schematic illustration of the orientation of the microscope view from the corneoscleral surface of the image captured in (B). In views from the corneoscleral surface, collector channel entrances leave SC above and below the plane of section making it difficult to assess SC, CCE and DSP relationships. **(D)** Schematic illustration of the orientation of the microscope view taken through the cut corneal surface in images of (E) and (F). The view through the cut

cornea captures the orientation of the CCE, and DSP adjacent to SC. **(E, F)** The red arrows identify locations where collector channel entrances arise from SC and connect with circularly oriented series of intrascleral channels coursing parallel to SC circumference (yellow arrows). The intrascleral channels communicate with one another providing a relatively continuous communicating ring. Blue arrows identify collecting vessels arising from the DSP that course radially through the sclera to the aqueous and episcleral veins on the surface of the eye. In the region between SC and the DSP running parallel to SC, a relatively thin layer of tissue is present (See Fig. 2, 8 & 9). The relatively long thin regions of tissue separating SC and the circularly oriented DSP are effectively hinged at their ends providing an anatomic relationship that ma provide the ability for the thin regions to move in response to IOP changes. (See Fig. 7–13) (A) is reproduced with permission from Hogan et al. (1971). [(B) non-human primate; m. nemestrina.] [(E) & (F); human.].

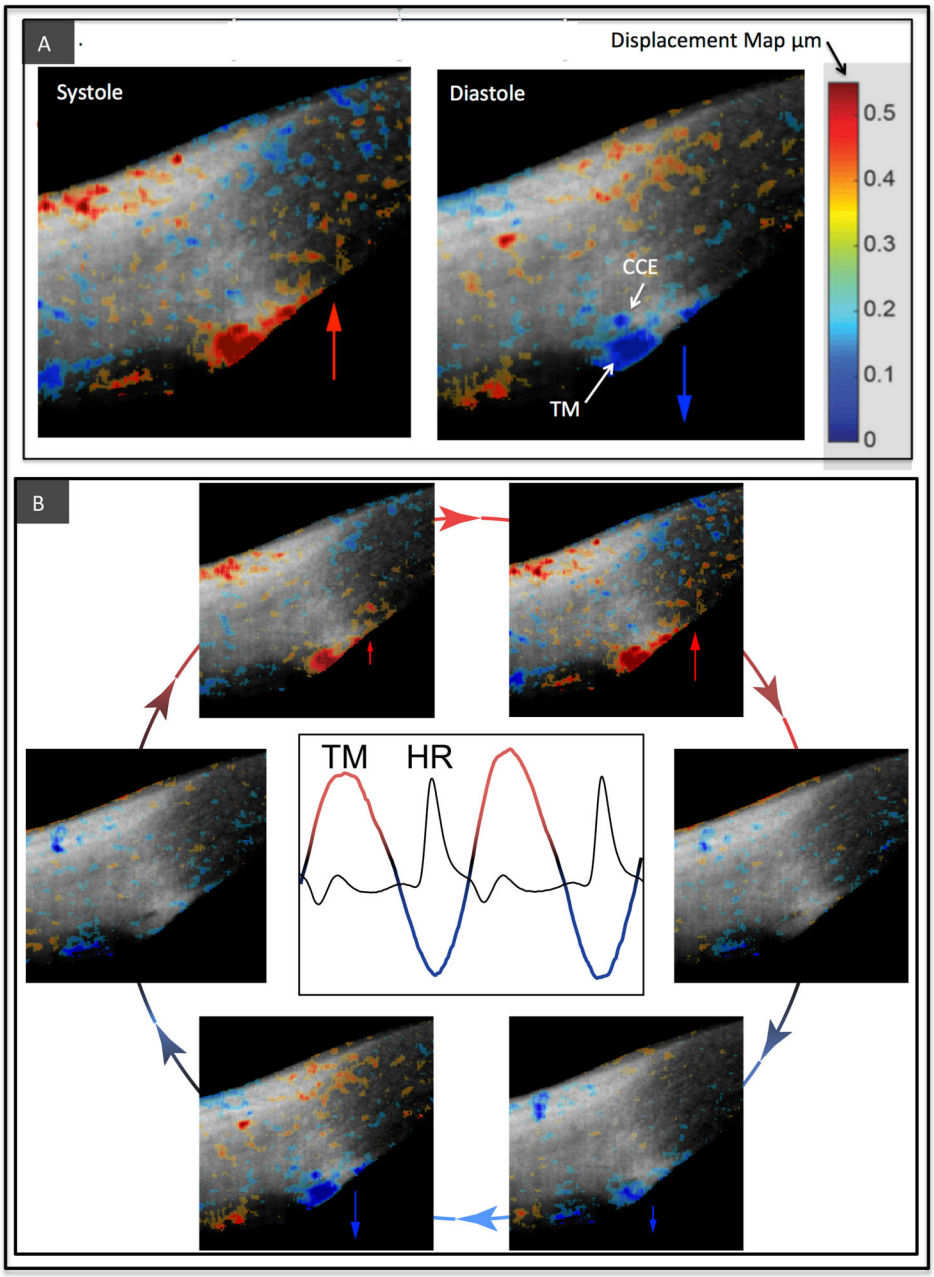

Fig. 3.

Data derived from imaging of cyclic, pulse-dependent tissue motion of the aqueous outflow system. **(A)** Live imaging of the aqueous outflow system in the temporal quadrant of the limbus of a normal human eye. The gray scale images are of structural details obtained by spectral domain optical coherence tomography (SD–OCT). Phase sensitive OCT (PhS–OCT) color displacement map information obtained from the same dataset is superimposed on the structural image and represents changes in displacement of trabecular meshwork (TM) and tissues surrounding collector channel entrances (CCE). The tissue motion results in lumen dimension changes of Schlemm's canal, CCE and intrascleral collector channels. The increasing intensity in red represents the increase of displacement of tissue motion

towards SC external wall and toward the sclera during systole when the pulse-induced IOP increases. Increasing intensity in blue indicates an increase of tissue displacement toward the anterior chamber during diastole when pulse-induced IOP decreases. **(B)** Arrows depict the image sequence around the periphery of the circle that encompasses one complete cardiac cycle. The central graph captures a tracing of trabecular meshwork (TM) bulk tissue motion over time using PhS-OCT. The heart rate (HR) tracing demonstrates that the TM motion is synchronous with the cardiac cycle but with a time delay. Reproduced with permission from Johnstone (2016).

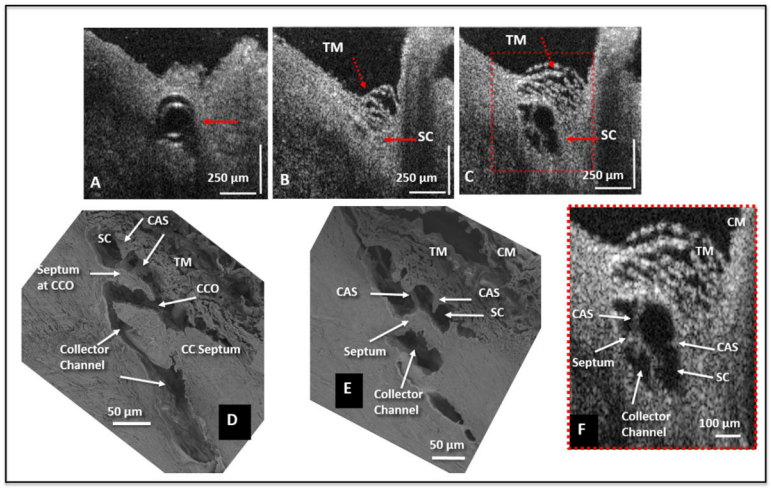

Fig. 4.

Representative two-dimensional (2-D) structural OCT and scanning electron microscopy images from the limbal region of an eye. **(A)** shows the OCT image captured with the cannula inside Schlemm's canal (SC) (arrow). The image location in **(B)** is ~150 µm away from the cannula tip and shows SC configuration before the infusion of perfusate. Arrows identify the TM and SC. In **(C)** the maximally dilated appearance of the same segment is visible after infusion of perfusate. (D) and (E) are representative SEM images from a radial limbal region, illustrating structural features of the outflow system that are mirrored in both the SEM and OCT images. **(D)** shows a collector channel entrance or ostia (CCO). A septum is present at the CCO that is attached to the TM by cylindrical attachment structures (CAS). **(E)** Is the adjacent section from the same segment showing the transition from the region of a CCO in (D) to a circumferentially oriented collector channel. **(F)** The 2X enlargement OCT image that is cropped from (C) permits a more detailed comparison of relationships. CM, ciliary muscle. Adopted from S. Hariri et al. Platform to investigate aqueous outflow system structure and pressure-dependent motion using high-resolution spectral domain optical coherence tomography. [non-human primate; M. nemestrina] Reproduced with permission from Hariri et al. (2014).

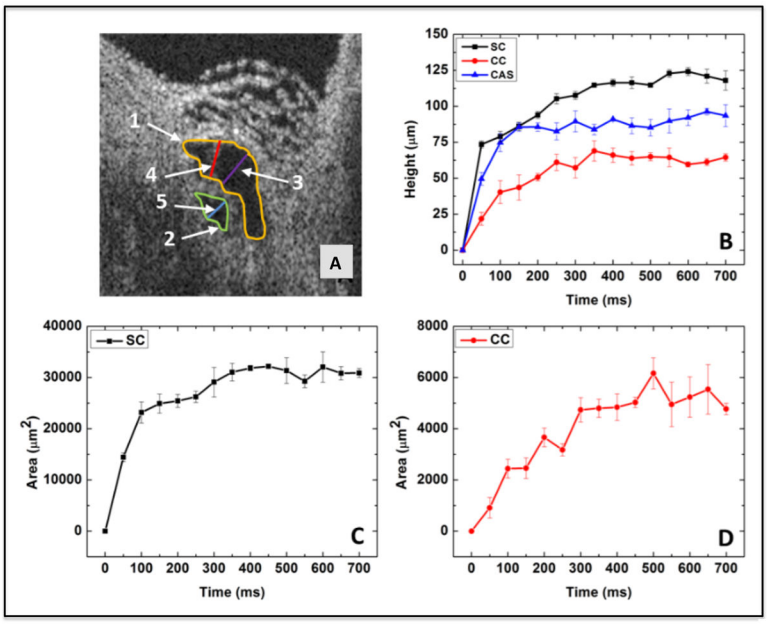

Fig. 5.

The 2-D OCT image from Fig. 11 and parameters derived from images. **(A)** SC and its adjacent collector channel (CC) are at their dilation maximum after a pulsed infusion. Parameters for quantification are shown: SC height, purple line; CC height, blue line; CAS height, red line; SC area, yellow line; CC area, green line. **(B)** Progressive increase in the height of SC (black curve), CC (red curve), and CAS (blue curve) with time. **(C)** The time-dependent change in SC lumen area. **(D)** The time-dependent change in CC lumen area. Height changes plateau in ~ 300 msec. Adopted from: S. Hariri et al. Platform to investigate aqueous outflow system structure and pressure-dependent motion using high-resolution spectral domain optical coherence tomography. J Biomed Opt 19(10) 106013. (2014) [non-human primate; m. nemestrina] Reproduced with permission from Hariri et al. (2014).

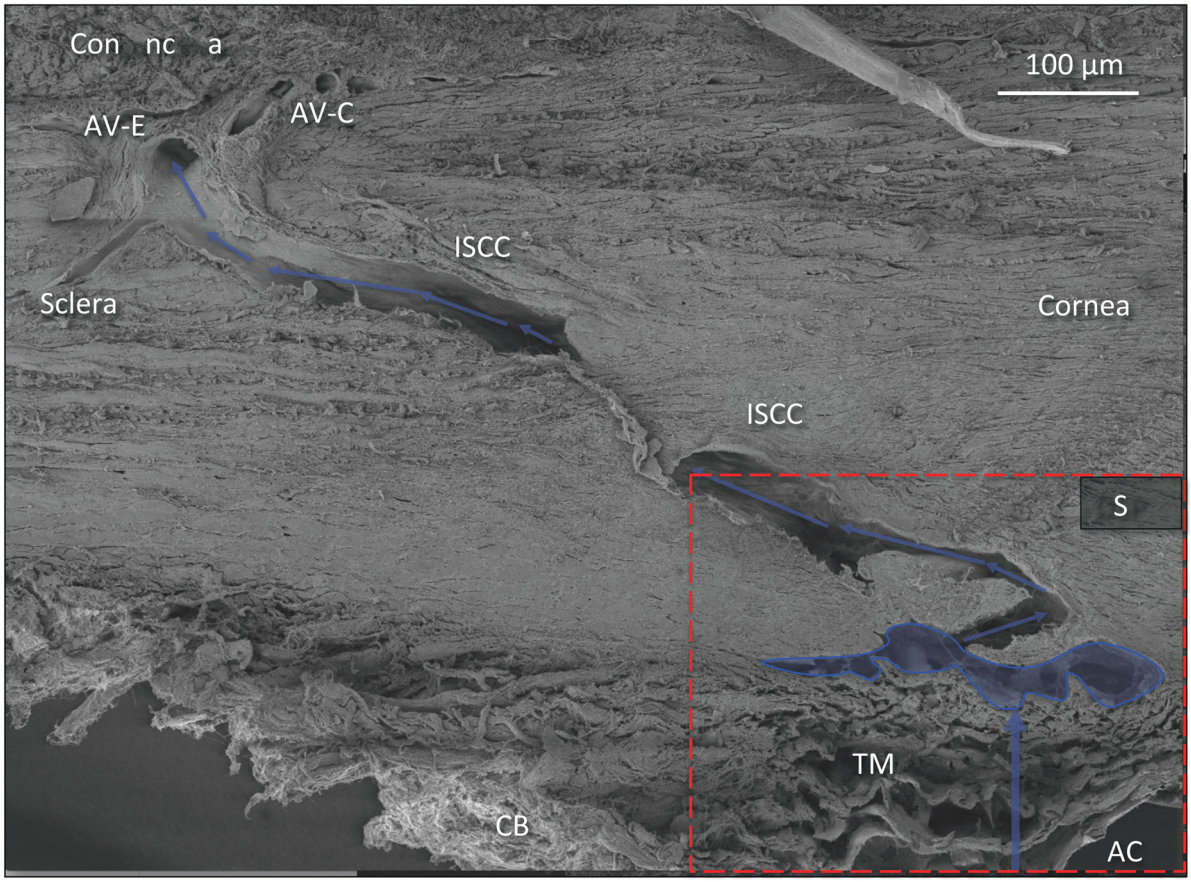

Fig. 6.

Pathway of Aqueous Humor: Scanning electron microscopy of aqueous outflow pathway from the anterior chamber (AC) through the trabecular meshwork (TM) to Schlemm's canal (outlined in blue). Blue arrows denote further aqueous passage through the deep intrascleral plexus (DSP) into the more superficial plexus of intrascleral collector channels (ISCC) Aqueous finally enters the episcleral (AV-E) and conjunctival (AV-C) aqueous veins. CB = ciliary body. Red dashed rectangle identifies region shown in Fig. 7. [non-human primate; m. nemestrina] Reproduced with permission from Johnstone (2016).

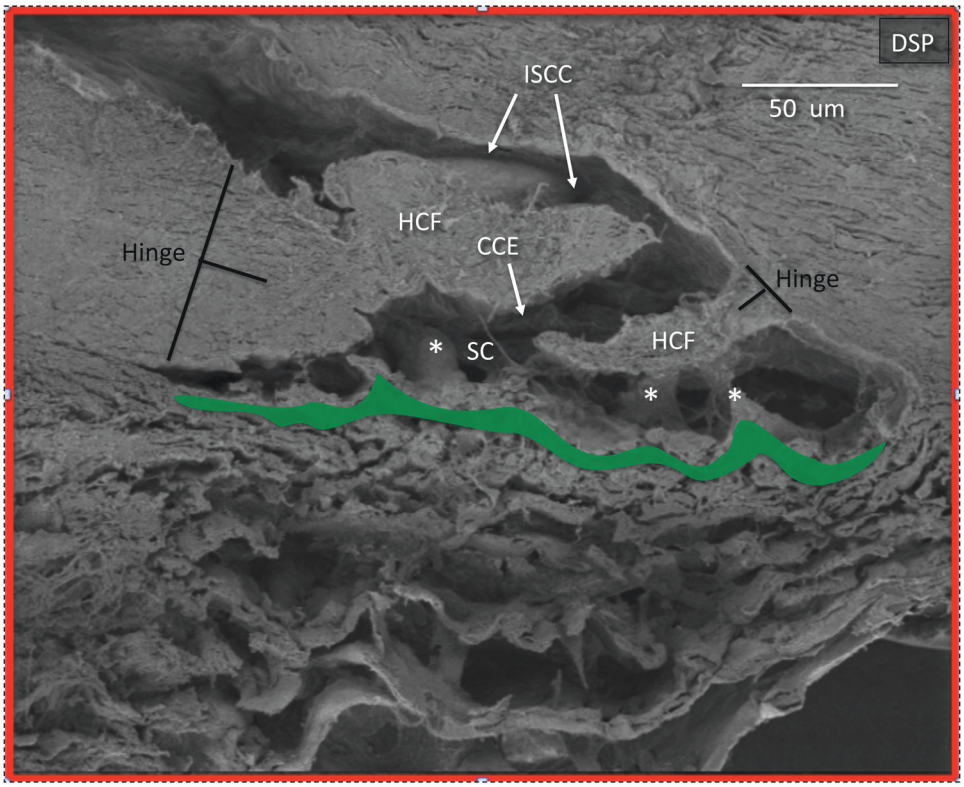

Fig. 7.

Collector channel and hinged collagen flaps or leaflets in deep scleral plexus: From area of Fig. 7 outlined in red. Schlemm's canal (SC) opens into a collector channel entrance (CCE). Collagen leaflets or flaps hinged at their scleral attachment (HCF) are present surrounding the convoluted pathway into the intrascleral collector channels (ISCC). Black T denotes the hinge locations. Area outlined in green denotes the juxtacanalicular space between the trabecular lamellae and SC inner wall. Cylindrical structures attach between SC inner wall and the HCF (*). If the TM moves, the HCF also will also move because of the connections between the structures. Reproduced with permission from Johnstone (2016).

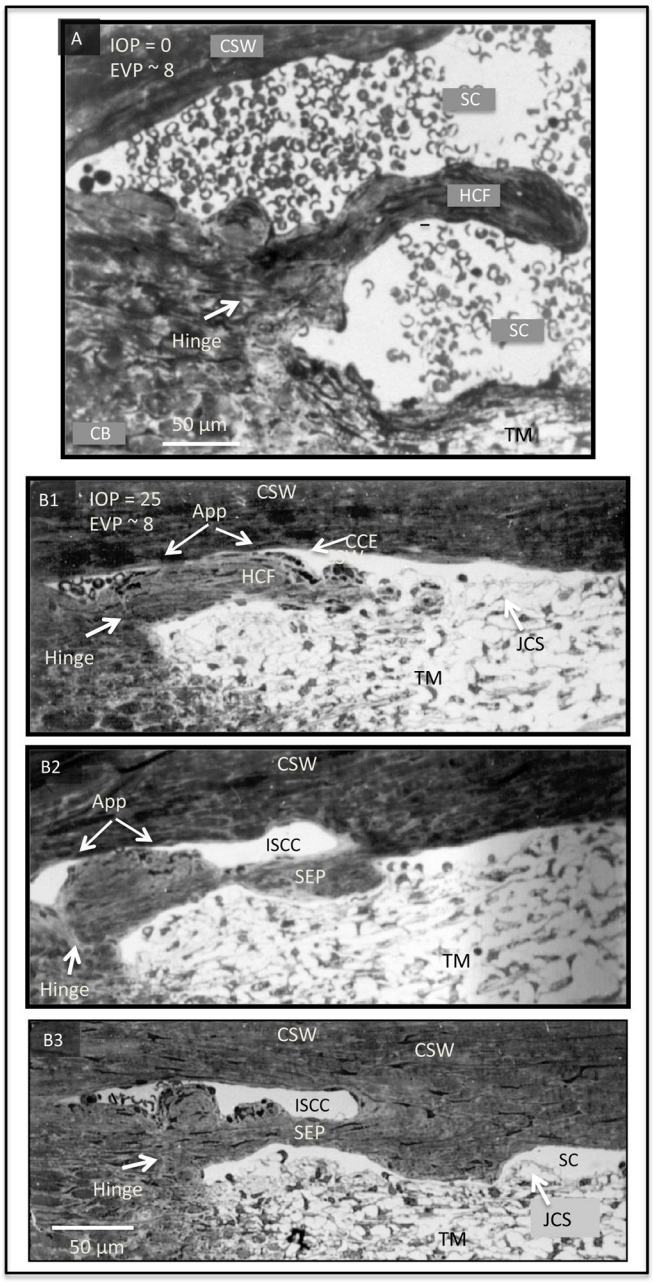

Fig. 8.

The ultrastructure of region around Schlemm's canal under various intraocular pressure (IOP). **(A)** IOP below episcleral venous pressure (EVP) during in vivo fixation. The trabecular meshwork (TM) is collapsed and far from the corneoscleral (CSW) of SC. Schlemm's canal (SC) is dilated and filled with blood. A collagenous flap-like structure continuous with the collagen lamellae of the sclera protrudes into SC. The flap is only attached or anchored at one end with the other end unattached creating a hinged flap arrangement (HCF). The HCF is far from SC external wall. **(B1)** IOP of 25 mm Hg during in vivo fixation. **(B2)** In additional serial sections the HCF of (A) developed an attachment to the corneoscleral wall thus developing into a septum (SEP) that creates an intrascleral

collector channel. **(B3)** In further serial sections, a more robust attachment developed between the SEP and the CSW. In each of the 3 images (B1–3), the TM is distended and SC is little more than a potential space with some areas of TM inner wall apposition to the corneoscleral wall of SC. A HCF at the entrance of the CCE was found in serial sections to be intermittently appositional (app) to SC external wall. Serial sections revealed that the SEP in (B) and (C) had intermittent areas of apposition to the CSW. At the hinge region (white arrows) a change in the orientation of the collagen lamellae of was regularly seen in serial sections. Reproduced with permission from Johnstone (2016). (non-human primate; M. mulatta).

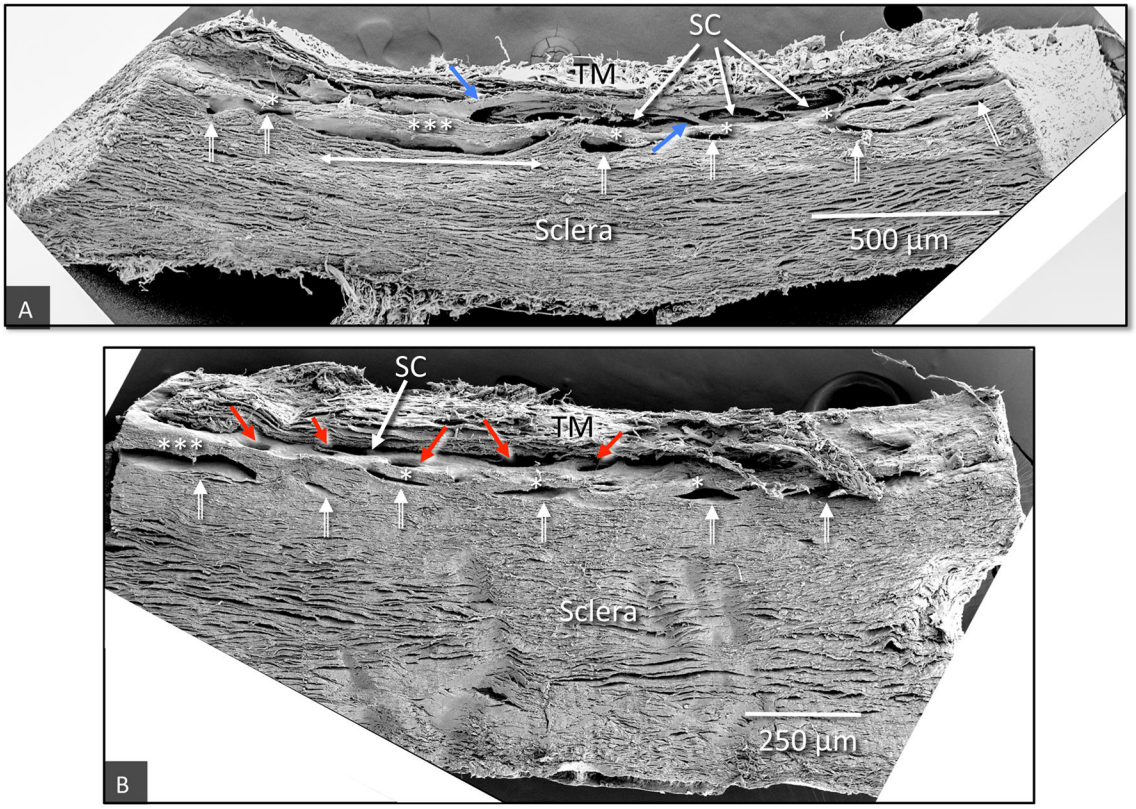

Fig. 9.

Scanning electron microscopy of tilted frontal sections providing images of regions of the limbal circumference that include the trabecular meshwork, (TM), Schlemm's canal (SC) and a series of intrascleral collector channels ISCC (white double bar arrows) in the deep scleral plexus. **(A)** The ISCC are distributed in a relatively narrow region close to SC. Rather than being round the ISCC have long dimensions' parallel to and a short dimension perpendicular to SC. The ISCC configuration results in thin septa (*), attached at their ends to the sclera that are at times have a length many times their height (***). Blue arrows identify cylindrical structures crossing SC that connect the trabecular meshwork with regions of SC external wall near CCE. **(B)** The collector channel entrances (CCE) are depicted by red arrows (non-human primate, M. fascicularis).

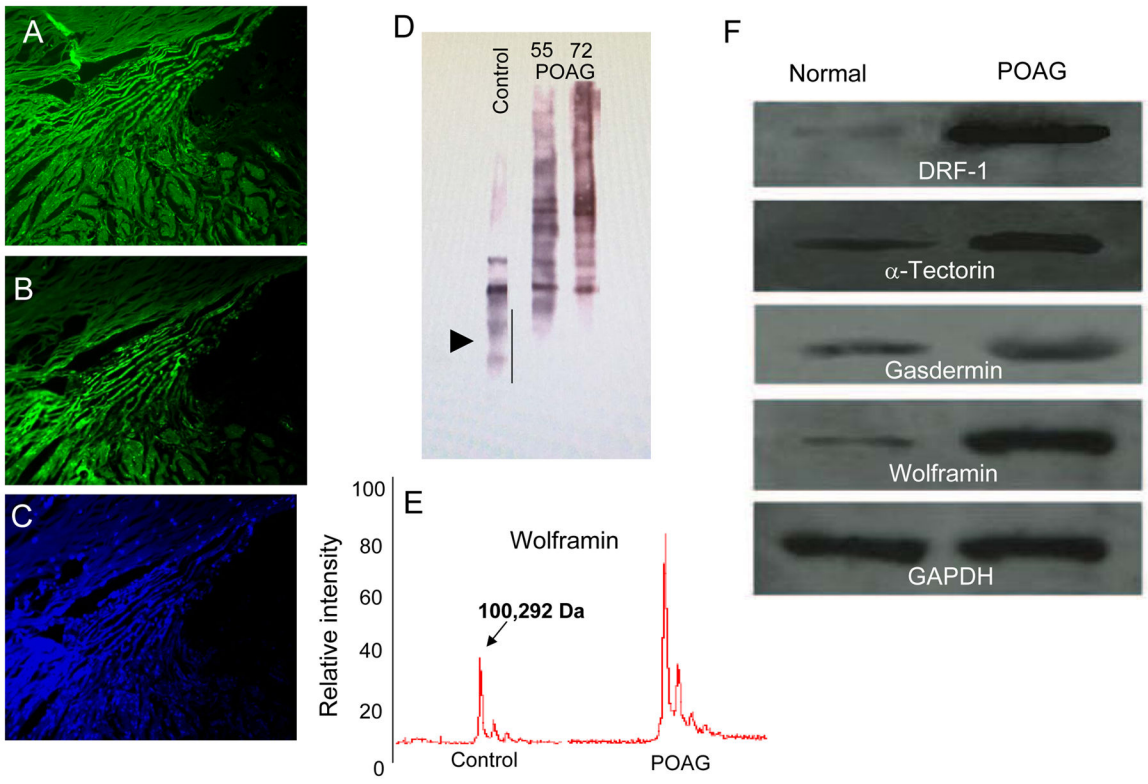

Fig. 10.

Assessment of basement membrane (BM) proteins in the trabecular meshwork (TM) region. **(A–B)** Probing consecutive sections of TM with different collagen IV antibodies shows different distribution patterns. **(C)** DAPI stained image of the same TM region. **(D)** Western blot analysis for type IV collagen demonstrates more fragmentation and less intact collagen IV in normal controls compared to POAG TM. **(E)** Linear mode MALDI-TOF analyses for Wolframin (WFS1) shows more intact protein in the POAG compared to control TM. **(F)** The GAPDH normalized levels for all proteins as indicated suggest more intact BM and BM interactors in the POAD TM compared to controls [adopted from Goel et al. (2012) PLoS One7(4): e34309].

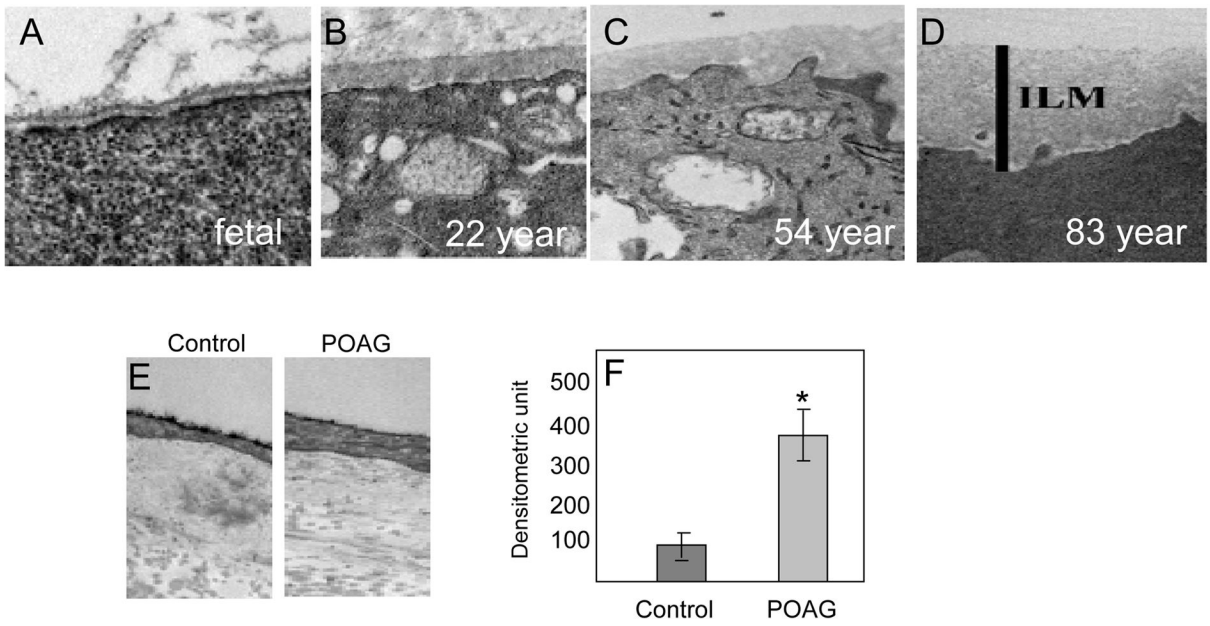

Fig. 11.

Basement membrane changes in ageing and glaucoma. **(A–D)** The basement membrane (BM) of inner limiting membrane (ILM) at the vitreoretinal surface of the retina undergoes a significant thickening due to ageing from fetal to 83-years-old as indicated. Adopted with permission from Candiello et al. (2010) Matrix Biology 29: 402–10. **(E)** The representative BM changes in the intra-trabecular space in transmission electron micrographs (TEM) en-bloc staining with uranyl acetate (Alcian Blue 8GX). As indicated, control (55-year-old) and primary open angle glaucoma (POAG; 55-year-old), both male cadaver donor eyes respectively. **(F)** Assessment of intra-trabecular BM thickness from 50 locations each from individual TEM images from 6 control and POAG donors each (age 55–59, equal distribution of genders). Asterisk indicate significance ($p<0.05$) using two-tailed equal variance t-test.

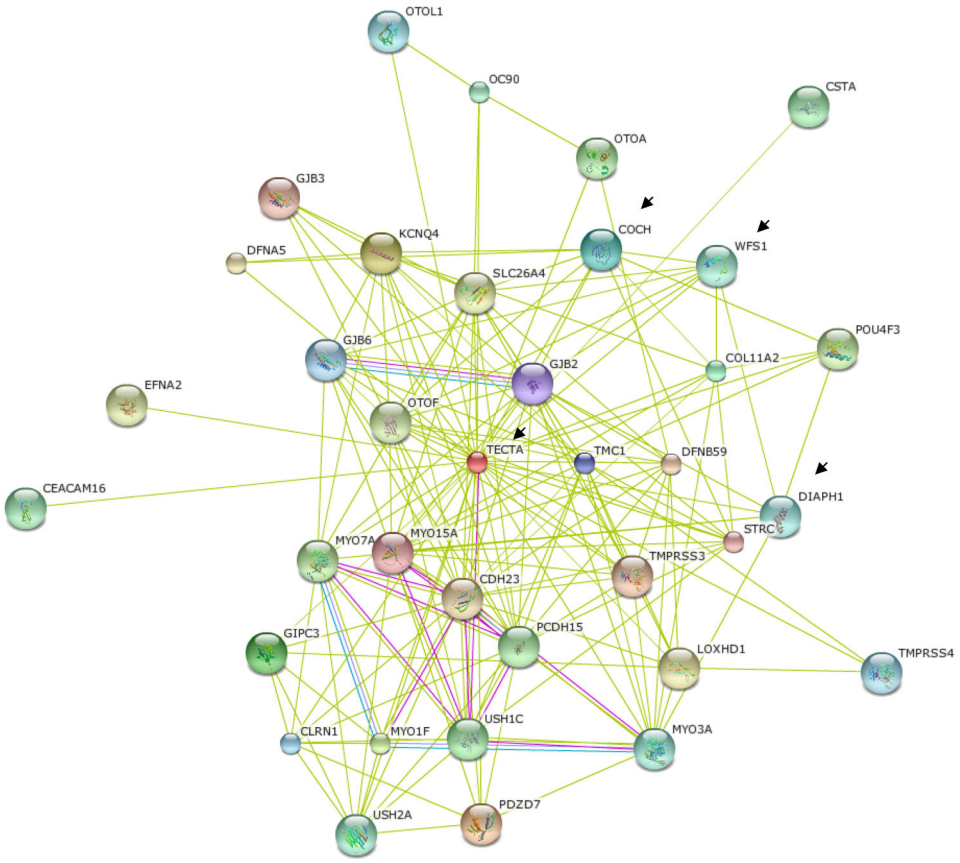

Fig. 12.

Potential in silico predicted interactors of cochlin including inner ear known basement membrane (BM) proteins. The balance of body depends on incremental movement of inner ear fluid. Such motions are often infinitesimally small in magnitude. In silico cochlin is predicted to interact with α-tectorin (TECTA), Wolframin 1 (WFS1), Diaphanous like formin-1 (DIAPH1 or DRF-1) as indicated by arrow. The α-tectorin is a bonafide BM protein of inner ear tectorial membrane some of its interactors have been recently predicted to be part of BM such as ruffle membranes. Mutation in WFS1, Gasdermin and DIAPH1 have been found to be associated with eye diseases.

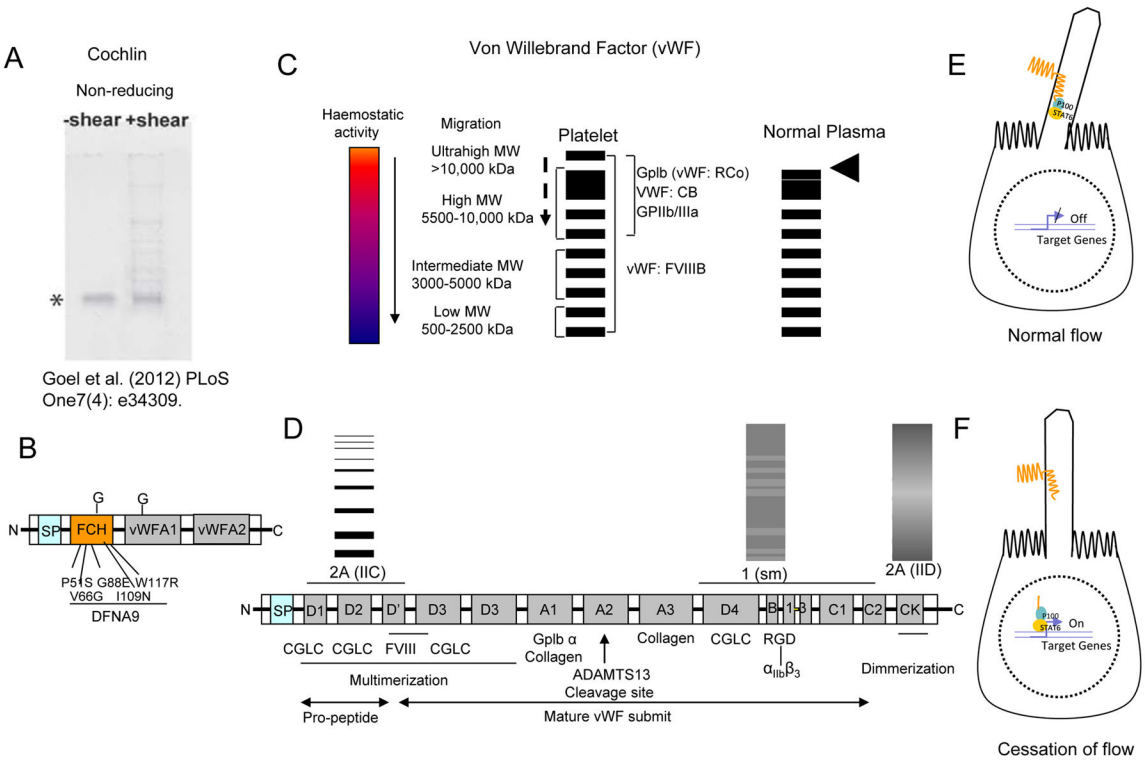

Fig. 13.

Solution phase mechanosensing in the Trabecular meshwork. **(A)** Multimerization of cochlin under shear stress and under non-reducing conditions [adopted from Goel et al. (2012) PLoS One7(4): e34309]. **(B)** The schematic depiction of domains in cochlin protein. The factor C homology domain (FCH) identified mutations have been shown to play in progressive hearing disease DFNA9, which is associated with inner ear fluid flow homeostasis. Two von willebrand factor A domains (vWFA1 &2) and glycosylation sites (G) are as indicated. **(C)** Schematic depiction of different von Willebrand factor (vWF) multimer sizes and their known role in hemostatic activity (the spectrum has been indicated; arrow indicates decreased activity). Ultralarge MW (ULMW) forms are found in platelet or endothelial cells but are absent in normal plasma (arrow head). Dashed arrow indicates decreased binding to proteins as indicated such as ricosetin (vWF: Rco) or collagen (vWF: CB). **(D)** The different vWF domains, their binding propensity with proteins and role in multimer formation. ADAMTS13 cleavage site as indicated. The multimers for three vWF disease conditions have been shown (1, 2A IIC and 2A IID). **(E, F)** Mechanosensing by polycystein1 (PC1) in kidney. **(F)** The truncated PC1enters nucleus and stops gene expression as a consequence of flow cessation.

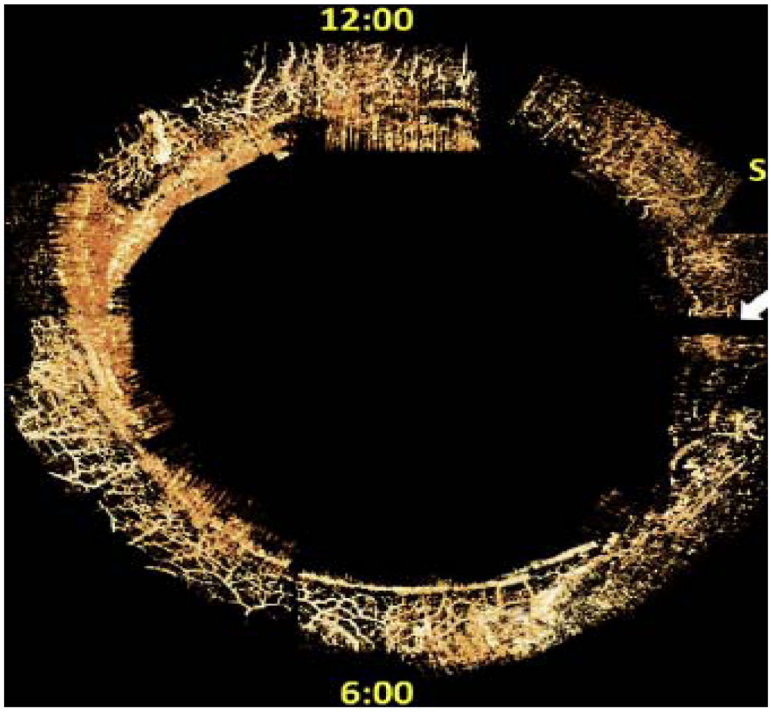

Fig. 14.

A representative optical coherence tomography image of distal outflow region in a human eye. Circumferential limbal scans in the original study were processed and assembled manually in 3D space to yield a full casting of the episcleral and intrascleral venous plexus throughout the limbus in-situ during active perfusion. Adopted with permission from Kagemann et al. Exp. Eye Res. (2011) 93 308–315.

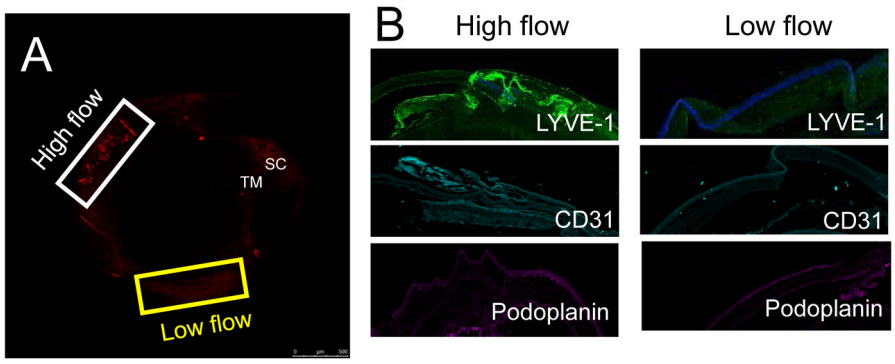

Fig. 15.

Distal outflow is likely to be impaired in pathologic state (glaucoma). **(A)** The DBA/2J hypertensive mouse shows regions of high and low flow, which is found to be associated with low and high elastic modulus respectively. Trabecular meshwork (TM) and Schlemm's canal (SC) located as indicated. **(B)** The adjacent regions of TM in DBA/2J hypertensive mouse demonstrates presence of elevated levels of vessel markers LYVE-1, CD31 and Podoplanin in high flow regions contrast to low flow as indicated. The distal flow regions in DBA/2J mouse are non-uniform. These regions have been shown to have high non-uniformity and abnormalities in human glaucoma subjects compared to controls.

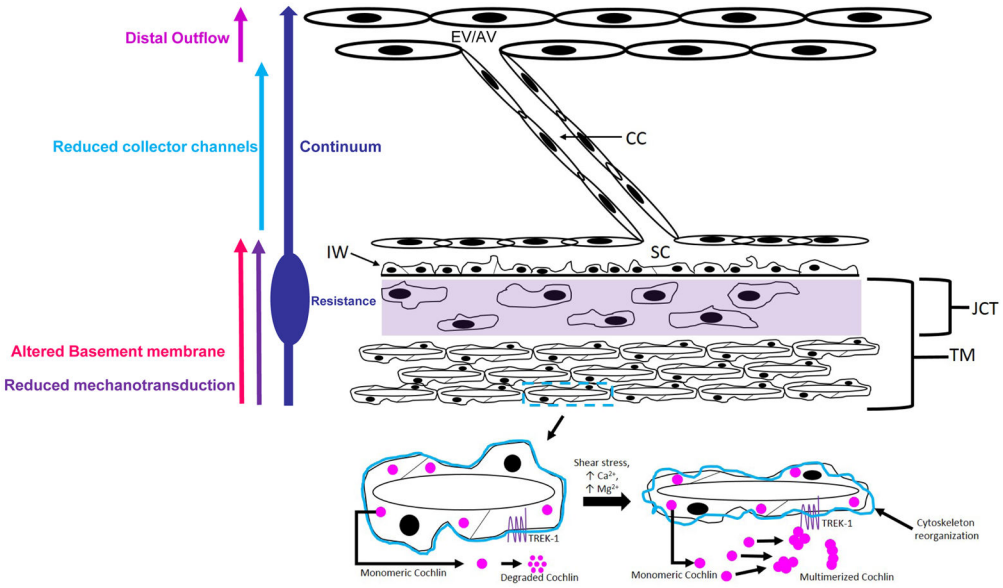

Fig. 16.

The proposed model of continuum. Reduced or altered mechanotransduction in the TM due to alteration of soluble mechanosensing molecules or their deposition results in pathology in the TM. At all levels of TM including Schlemm's canal (SC), the basement membrane degradation is impaired resulting in lack of generation of pro- and anti-angiogenic molecules such as endostatin, canstatin, tumstatin fragments of type IV collagen. There is observed reduced collector channel (CC) frequency and/or dimension in the surrounding region of TM. The fine regulation of degraded protein fragments of BM may be involved in regulation of CCs and distal flow regions. The model supports an integrated pathology encompassing TM, SC, CCs and distal outflow regions. JCT= juxtacanalicular tissue, IW inner wall of SC, AV = aqueous veins, EV= episcleral vein.

Table 1

Proteases identified with cochlin degradation activity

Class	Name	UniProt Accession number	Quantitative Proteomics	Immunoprecipitation	Qualitative Proteomics	Yeast 2 Hybrid
Aspartyl						
	Cathepsin D	P07339	Yes		Yes	
Metalloprotease						
	Glutamyl aminopeptidase	Q07075	Yes			
	Arginyl aminopeptidase	Q9H4A4	Yes			
	Stromelysin 2 (MMP10)	P09238	Yes			
	MMP17	Q9ULZ9	Yes			
	ADAM2/Fertilin-b	Q99965		IP-PrecipHen		
	ADAMTS2	O95450		IP-CRH		Yes
	Carboxypeptidase D	O75976	Yes	IP-CRH		
	ADAMTS4	O75173	Yes			
	ADAM19	Q9H013	Yes			
	Pappalysin-2	Q9BXP8				Yes
Serine						
	Plasminogen	P00747	Yes			
	Lactotransferrin	P02788			Yes	
	Proprotein convertase subtilisin/kexin type 9	Q8NBP7		IP-CRH		

Swiss-Prot database accession numbers are shown as well as the class of each protease. Proteases identified with quantitative and qualitative proteomics were done using iTRAQ 8-plex with 4 normal human TM samples followed by 4 glaucomatous human TM samples. Proteases identified with immunoprecipitation were done with PrecipHen by Aves Labs, Inc. or Catch and Release (CRH) immunoprecipitation kit. Proteins identified with yeast 2 hybrid system used pGBKT7-hCochlin as bait and a pGADT7-hBrain library.

Table 2

Future questions for investigation

1	Evidence documents pulse-dependent TM motion both ex vivo and in vivo in humans in synchrony with the ocular pulse. What studies are needed to determine whether such motion is reduced or eventually becomes absent in glaucoma?
2	Recent reports also document the presence of flap-like structures or leaflets at collector channel ostia that undergo motion. What studies are needed to determine whether CCE entrance motion is lost in glaucoma?
3	Connections between the TM and hinged CCE entrance flaps provide a mechanism to provide synchrony of motion of the TM and the CCE hinged flaps. The connections may also provide a mechanism to hold the CCE open as suggested by Rohen. What studies are needed to determine whether disruption of TM-CCE connections such as occurs in microsurgical procedures may lead to collapse of CCE?
4	Is the entire composition of the outflow system such as the TM, JCT, and SCE in the proximal system as well as CCE, ISCC, AV and ESV walls in the distal system a continuum designed to unify control of outflow homeostasis and IOP? What studies can be d0signed to demonstrate the continuity of mechanosensory mechanisms throughout the system?
5	What further studies would be useful to anlayze the molecular composition of proximal and distal outflow system structures to better characterize the functional role of molecules in these regions?
6	How does the molecular composition enable continuous motion of the TM and collector channel region? What studies may be undertaken to determine whether motion is important for continuous functional homeostasis in these regions?
7	Studies may be able to determine whether the molecular changes in the proximal outflow regions (TM,SC) induce molecular changes in the distal outflow regions that result in alterations in structure. Do proximal signals affect distal structural features normally or more specifically during the course of progression of pathology?
8	While the TM and SC are undergoing dynamic changes, could the downstream distal collector channels also undergo compensatory dynamic changes to maintain homeostasis? What studies could be designed to test the hypothesis?
9	Fluid flow in the AH outflow system is of much lower magnitude than in many other regions of the body. Is the complex nature of the outflow system a result of design needs for lower fluid flow regimes? What studies could be designed to test the hypothesis?